nature portfolio

https://doi.org/10.1038/s41586-022-05032-1

Supplementary information

Aligned macrocycle pores in ultrathin films for accurate molecular sieving

In the format provided by the authors and unedited

Supplementary Information

Aligned macrocycle pores in ultrathin films for accurate molecular sieving

Zhiwei Jiang[1,2,7], Ruijiao Dong[1,3,7], Austin M. Evans[4,5], Niklas Biere[6], Mahmood A. Ebrahim[1], Siyao Li[1], Dario Anselmetti[6], William R. Dichtel[4], Andrew G. Livingston[1,2]*

Affiliations:

[1]Barrer Centre, Department of Chemical Engineering, Imperial College London, South Kensington Campus, London SW7 2AZ, UK.

[2]Department of Engineering and Materials Science, Queen Mary University of London, Mile End Road, London E1 4NS, UK.

[3]Shanghai Centre for Systems Biomedicine, Key Laboratory of Systems Biomedicine (Ministry of Education), Shanghai Jiao Tong University, Shanghai, 200240, China.

[4]Department of Chemistry, Northwestern University, Evanston, IL 60208, USA.

[5]George & Josephine Butler Polymer Research Laboratory, Center for Macromolecular Science & Engineering, Department of Chemistry, University of Florida, Gainesville, FL 32611, USA.

[6]Experimental Biophysics and Applied Nanoscience, Faculty of Physics, Bielefeld University, 33615 Bielefeld, Germany.

[7]These authors contributed equally to this work.

*Correspondence to: a.livingston@qmul.ac.uk

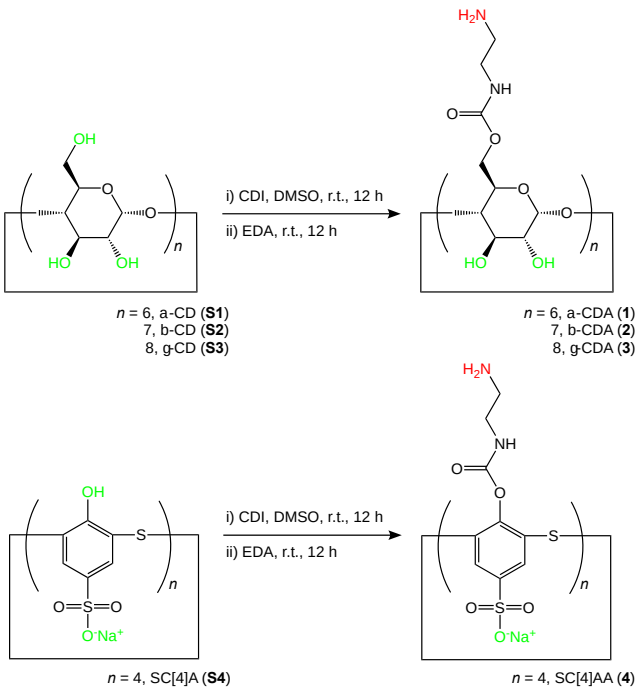

Supplementary Figure 1 | Synthesis of amino-functionalised macrocyclic derivatives including α-CDA (1), β-CDA (2), γ-CDA (3), and SC[4]AA (4).

NMR spectra

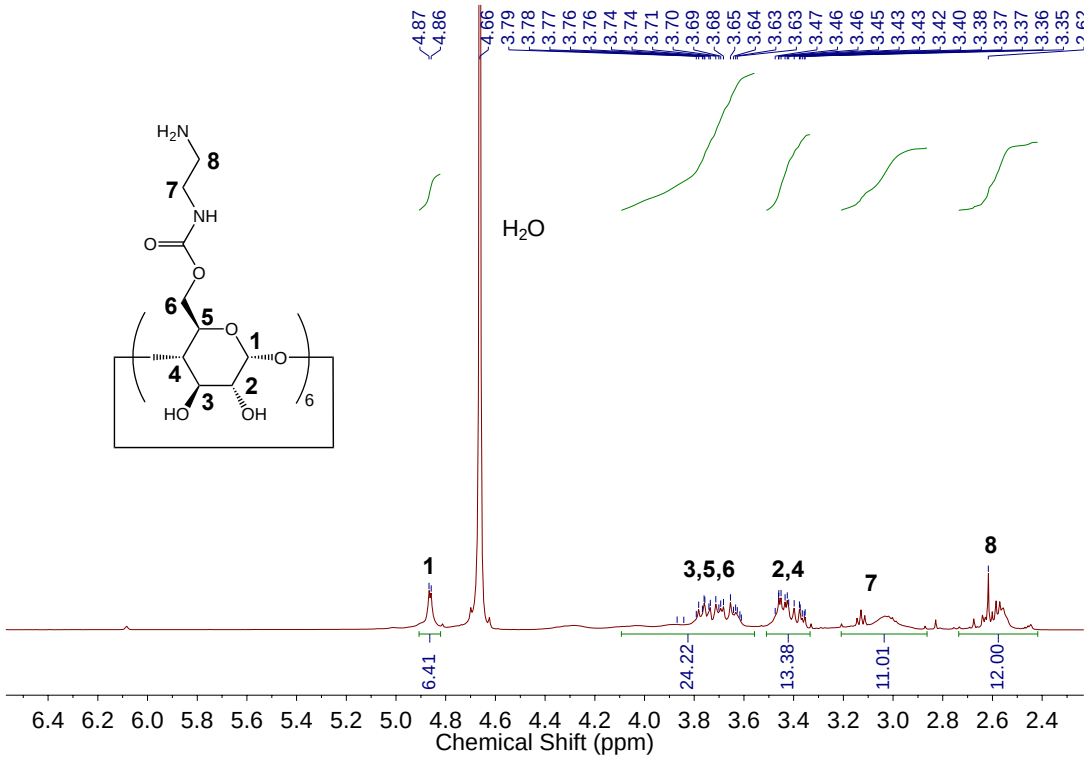

Supplementary Figure 2 | ^{1}H NMR spectrum of α-CDA (1) in D_2O.

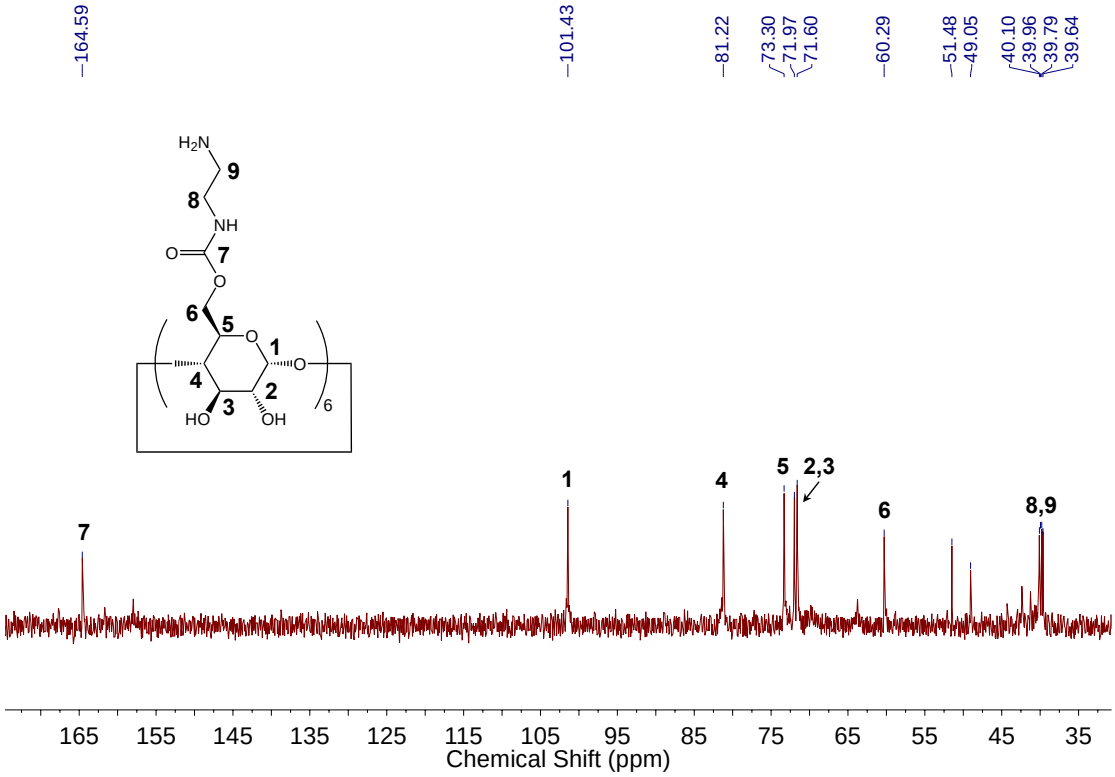

Supplementary Figure 3 | ^{13}C NMR spectrum of α-CDA (1) in D_2O.

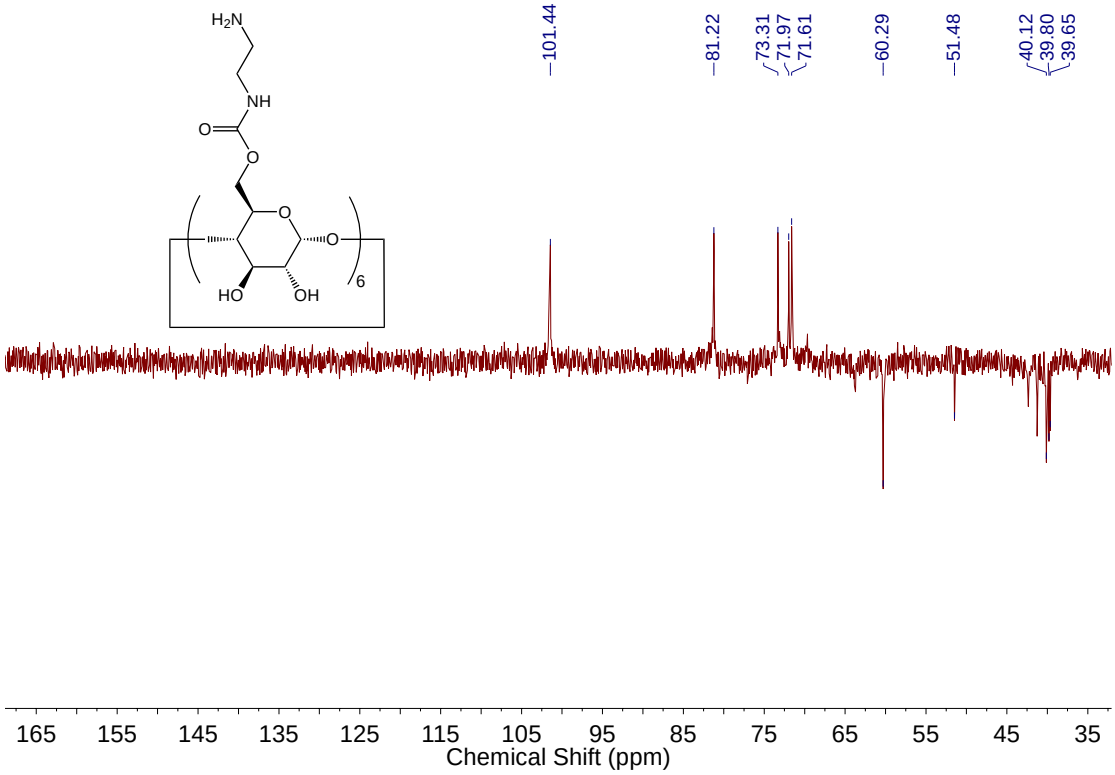

Supplementary Figure 4 | ^{13}C DEPT-135 NMR spectrum of α-CDA (1) in D_2O.

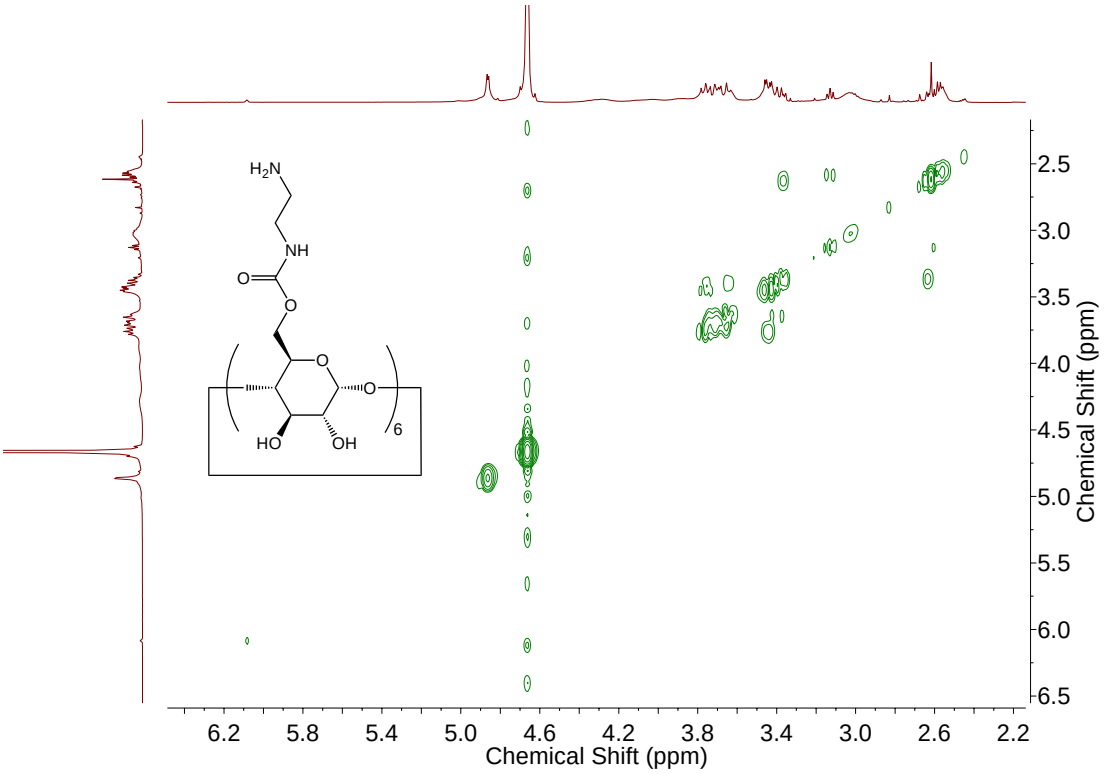

Supplementary Figure 5 | 2D ^{1}H-^{1}H COSY NMR spectrum of α-CDA (1) in D_2O.

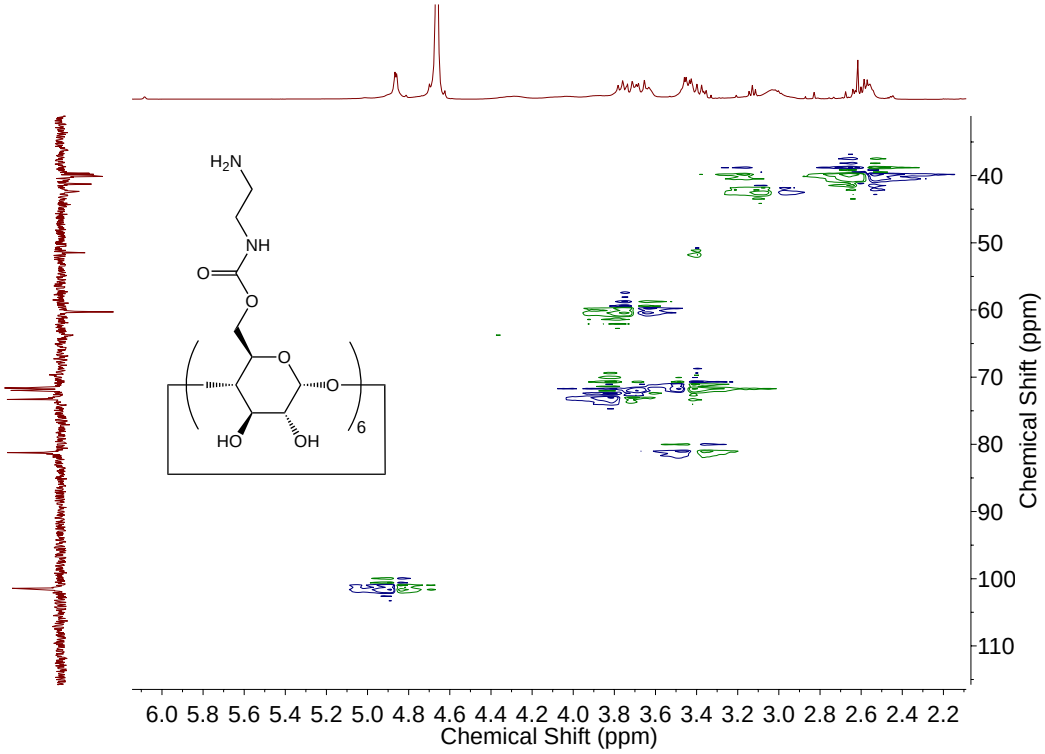

Supplementary Figure 6 | 2D ^{1}H-^{13}C HSQC NMR spectrum of α-CDA (1) in D_2O.

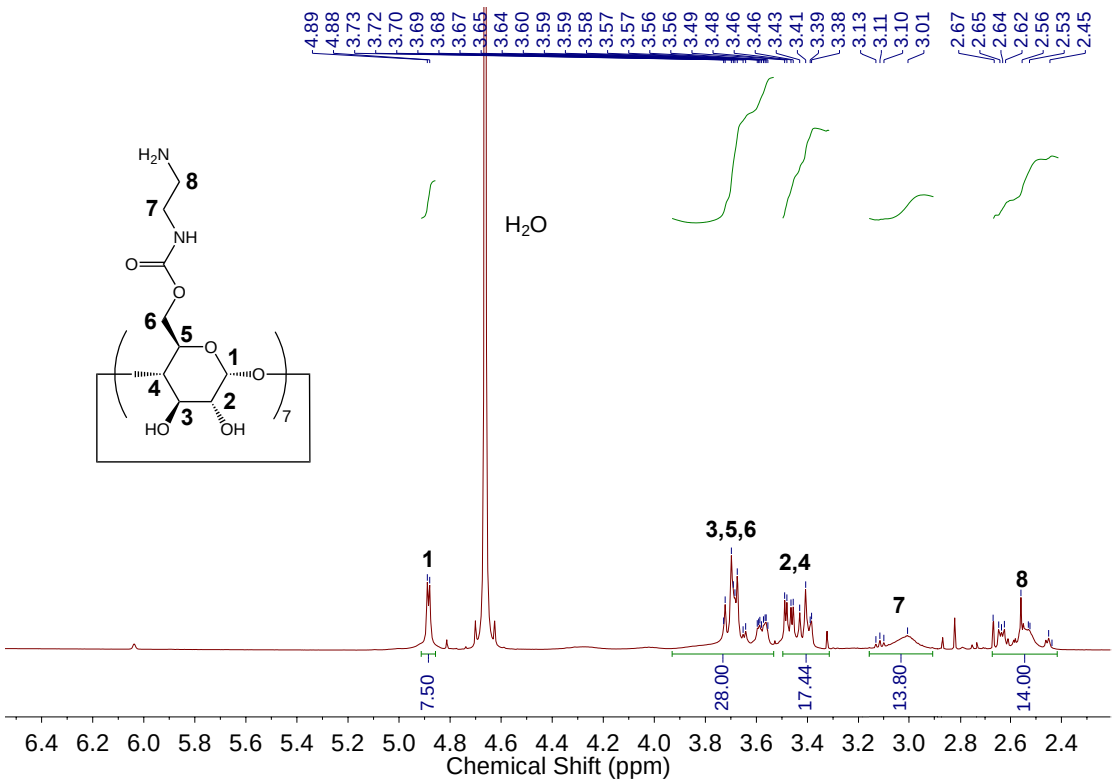

Supplementary Figure 7 | ^{1}H NMR spectrum of *β*-CDA (2) in D_2O.

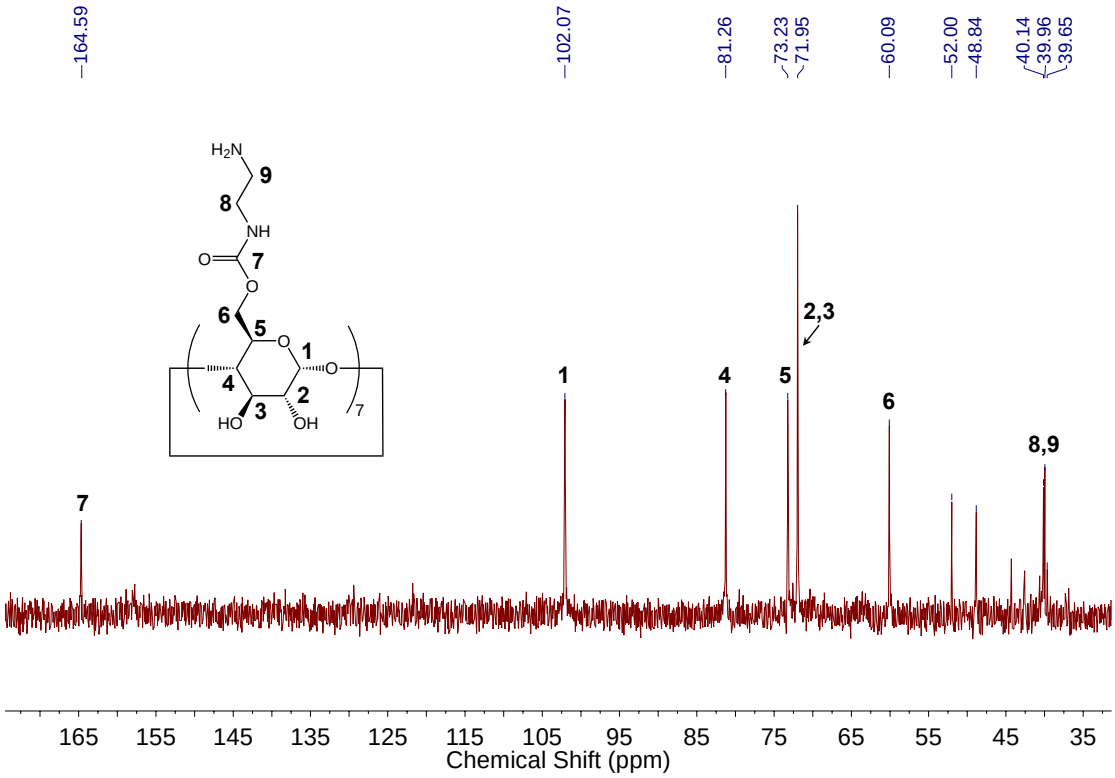

Supplementary Figure 8 | ^{13}C NMR spectrum of *β*-CDA (2) in D_2O.

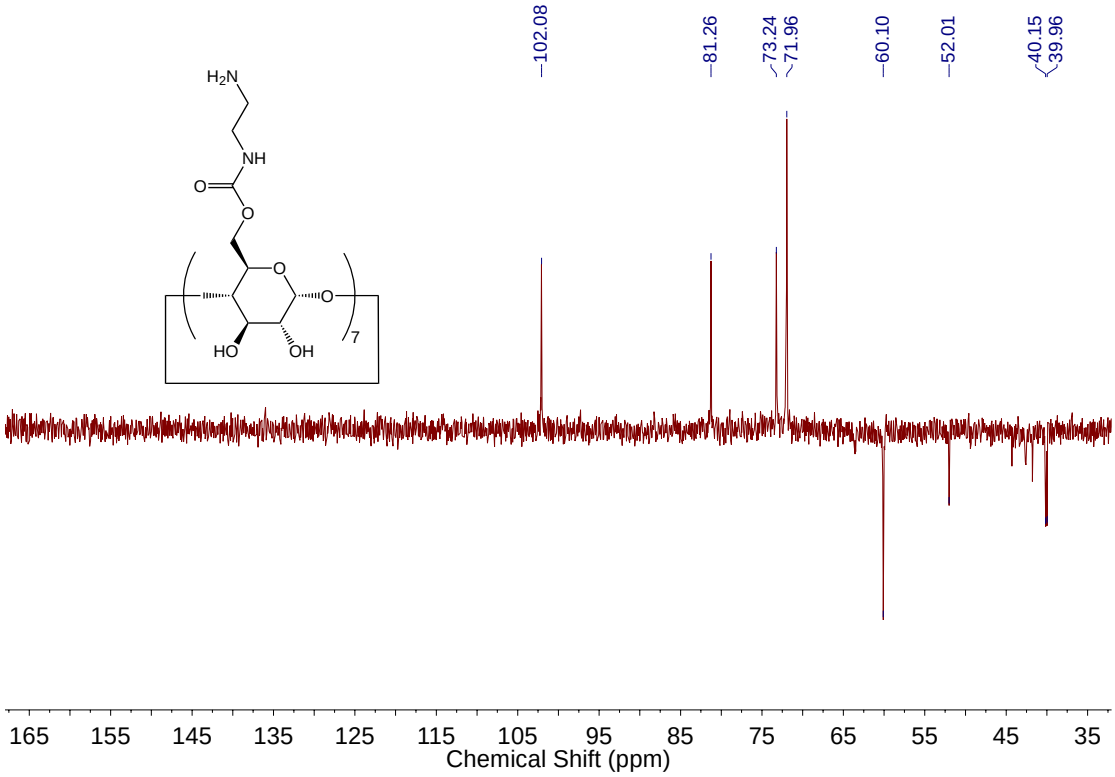

Supplementary Figure 9 | ^{13}C DEPT-135 NMR spectrum of *β*-CDA (2) in D_2O.

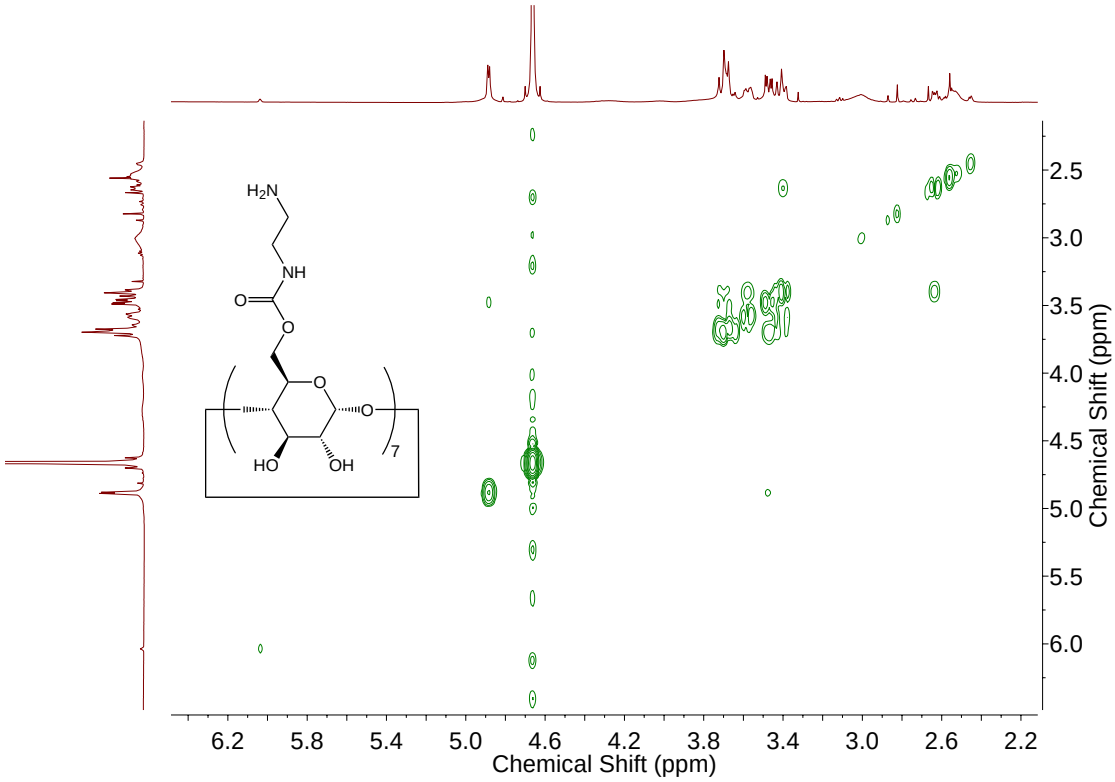

Supplementary Figure 10 | 2D ^{1}H-^{1}H COSY NMR spectrum of *β*-CDA (2) in D_2O.

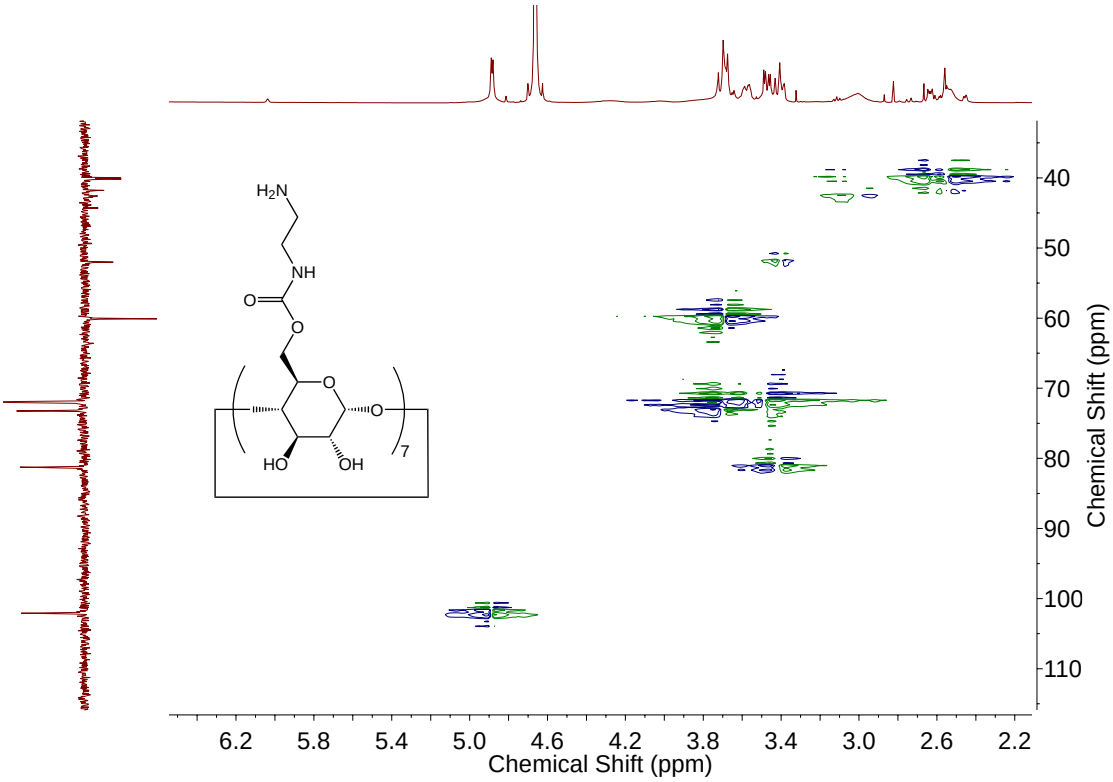

Supplementary Figure 11 | 2D ^{1}H-^{13}C HSQC NMR spectrum of *β*-CDA (2) in D_2O.

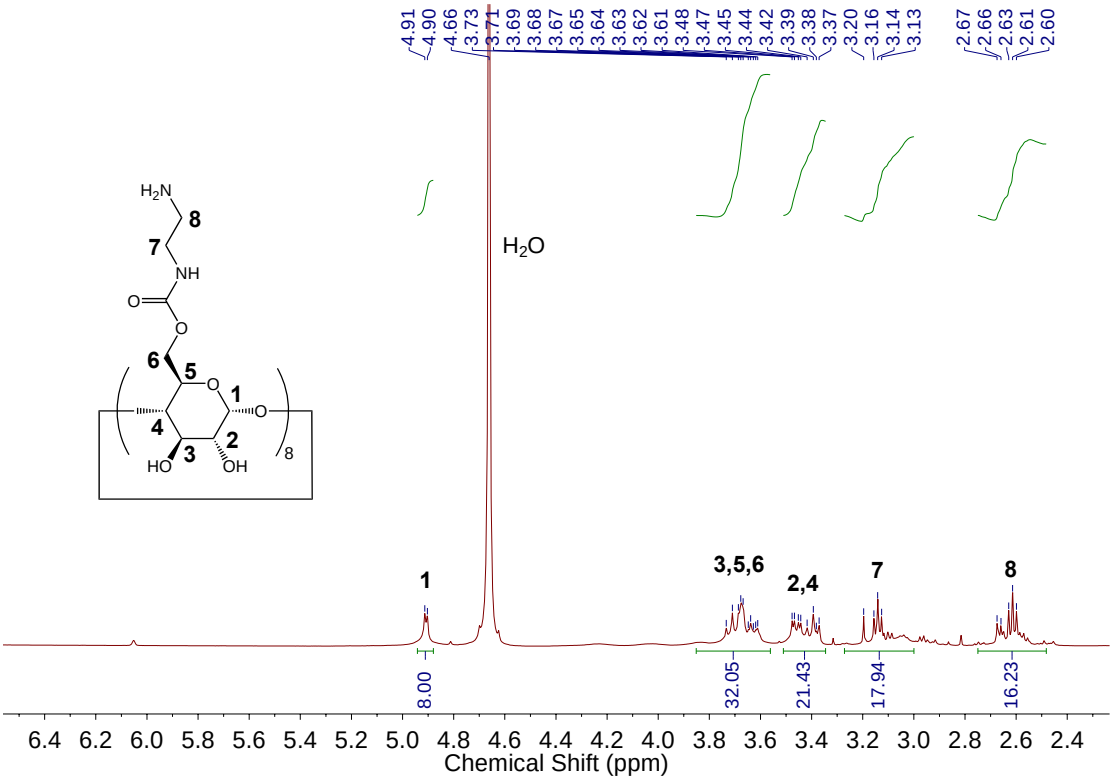

Supplementary Figure 12 | ^{1}H NMR spectrum of *γ*-CDA (3) in D_2O.

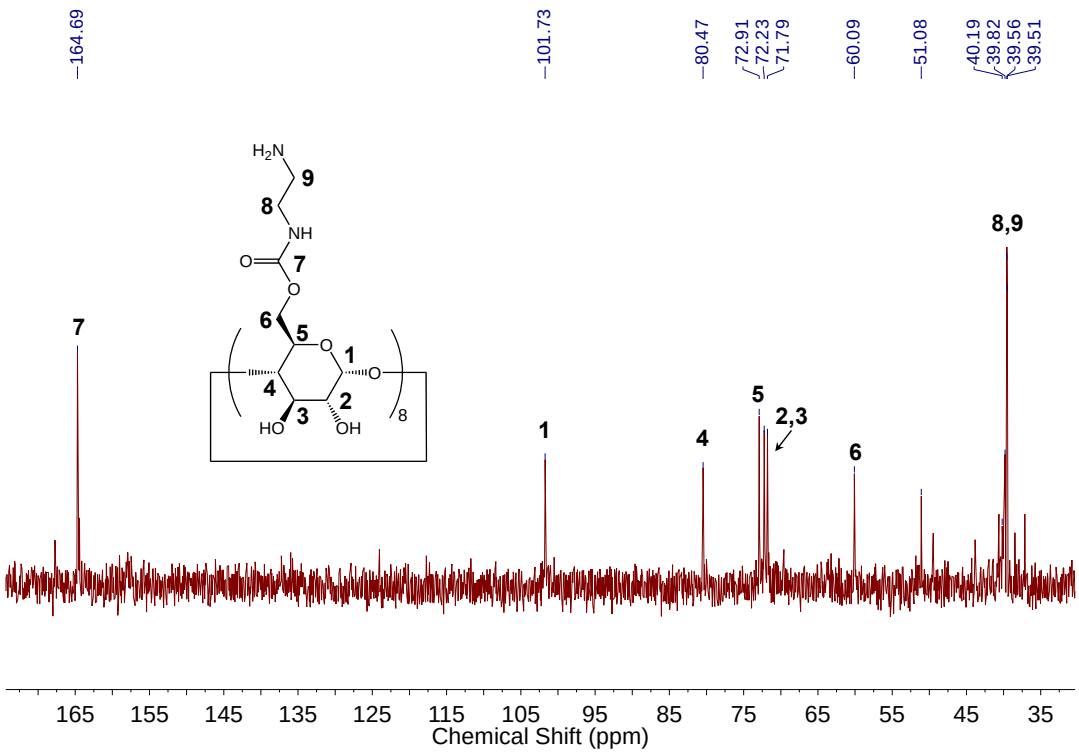

Supplementary Figure 13 | ^{13}C NMR spectrum of γ-CDA (3) in D_2O.

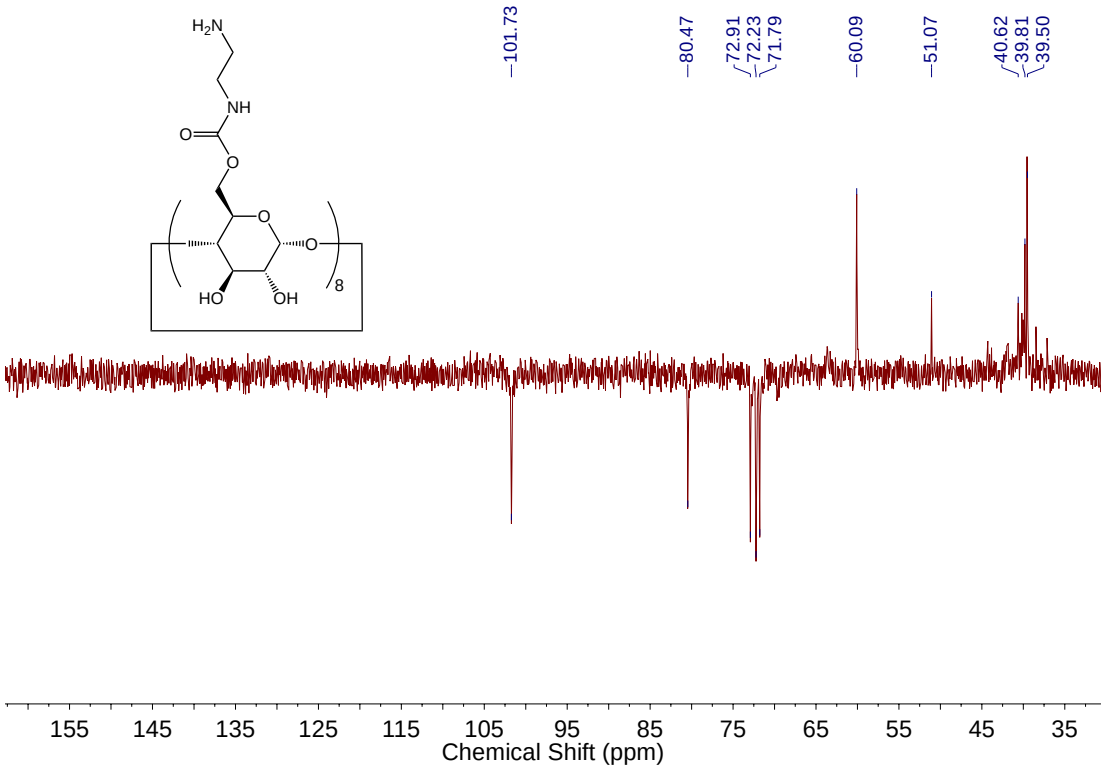

Supplementary Figure 14 | ^{13}C DEPT-135 NMR spectrum of γ-CDA (3) in D_2O.

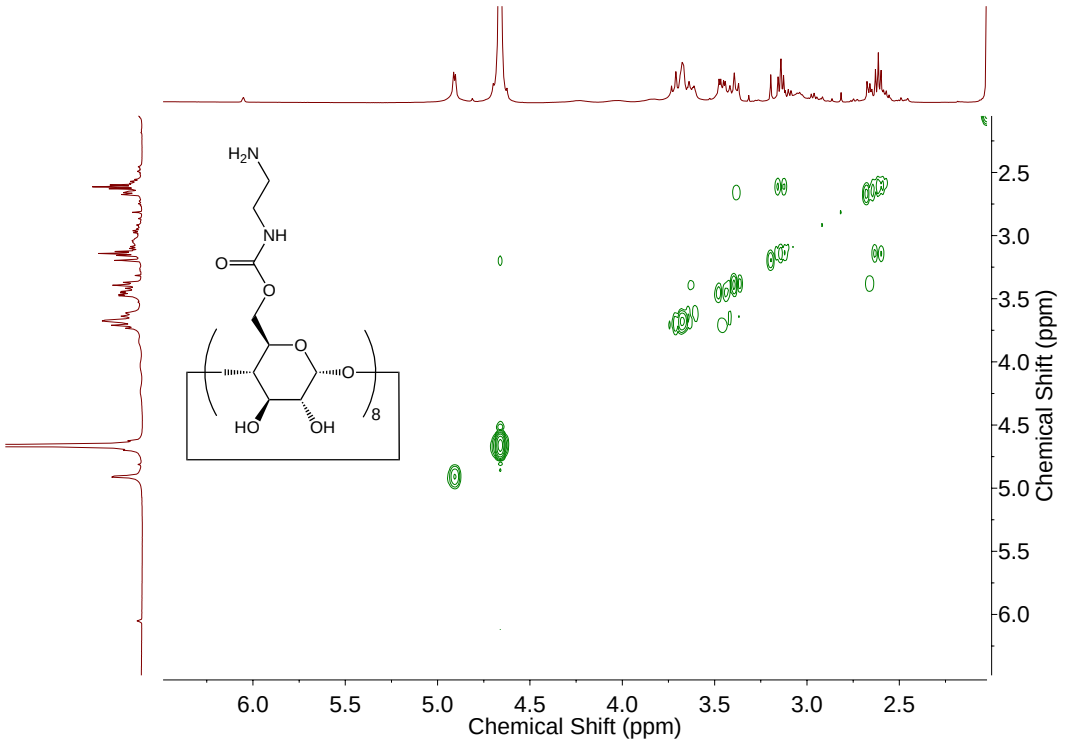

Supplementary Figure 15 | 2D ^{1}H-^{1}H COSY NMR spectrum of γ-CDA (3) in D_2O.

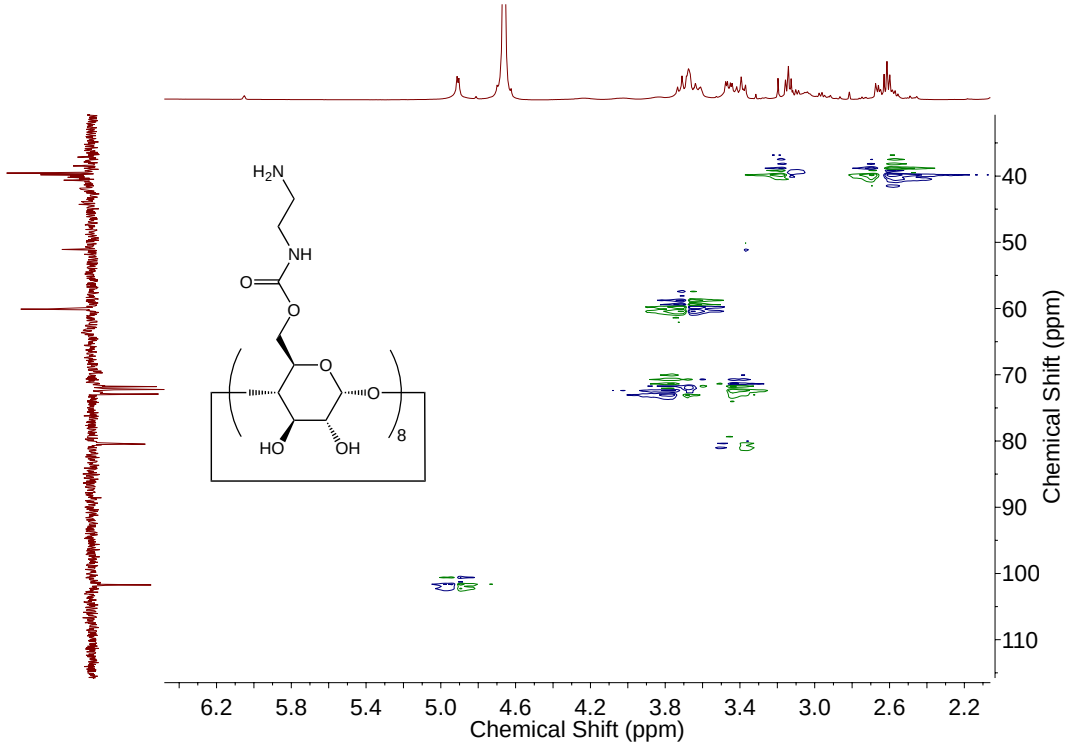

Supplementary Figure 16 | 2D ^{1}H-^{13}C HSQC NMR spectrum of γ-CDA (3) in D_2O.

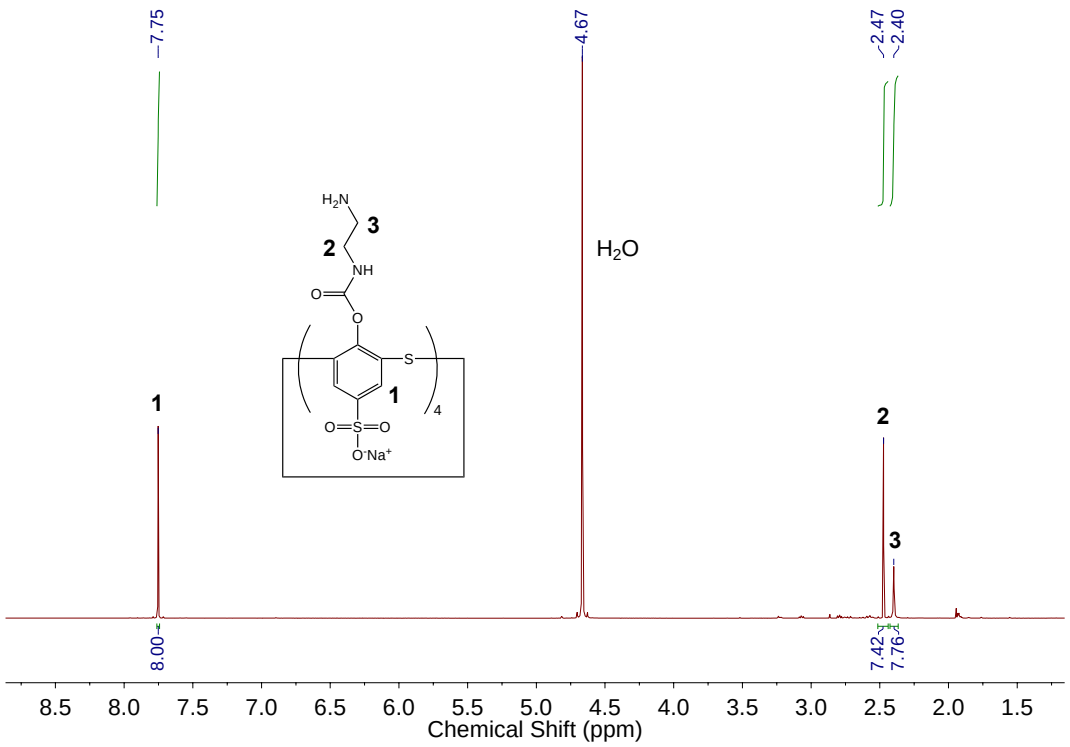

Supplementary Figure 17 | ^{1}H NMR spectrum of SC[4]AA (4) in D_2O.

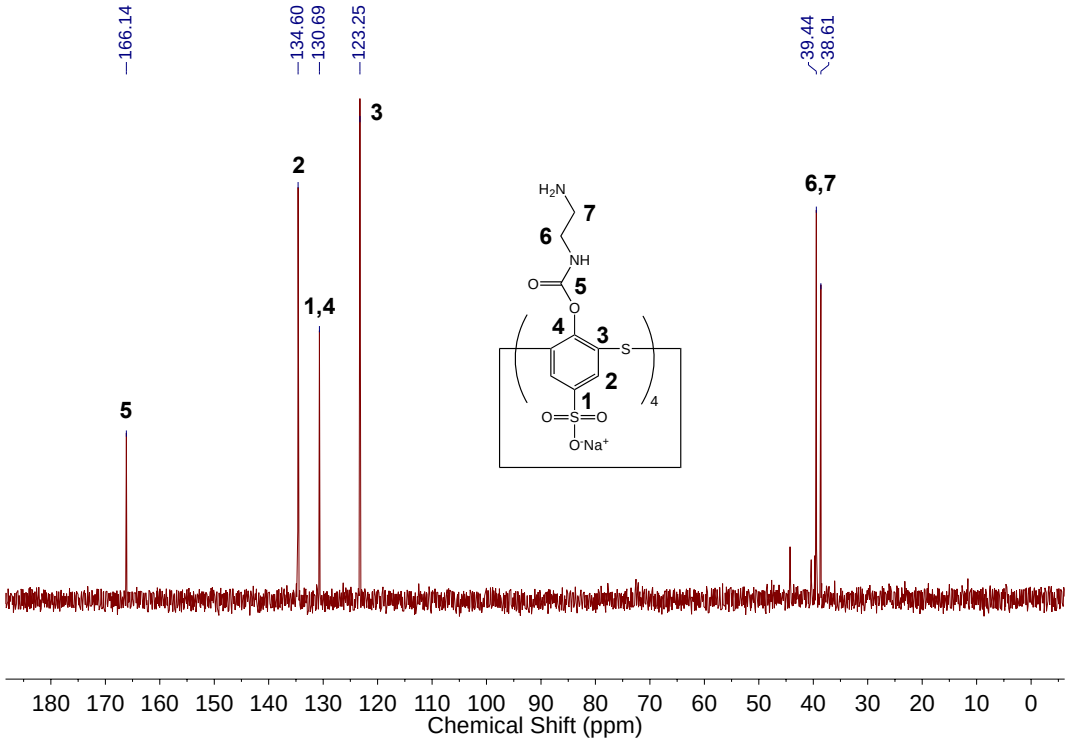

Supplementary Figure 18 | ^{13}C NMR spectrum of SC[4]AA (4) in D_2O.

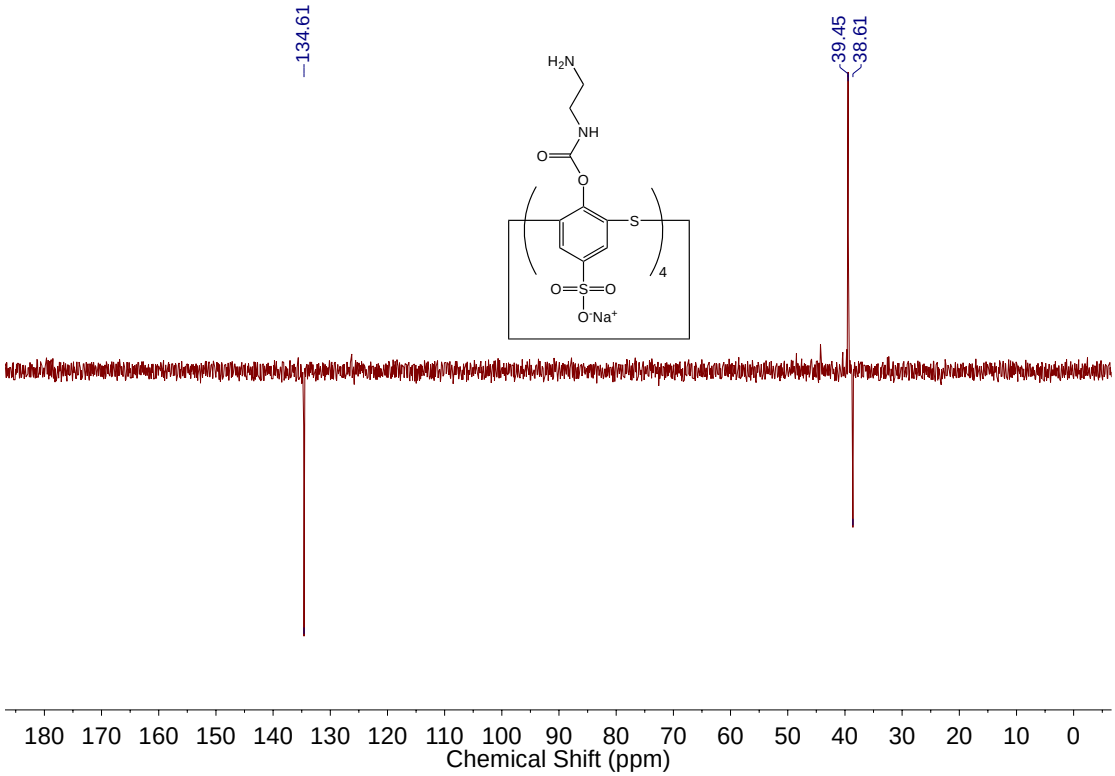

Supplementary Figure 19 | ^{13}C DEPT-135 NMR spectrum of SC[4]AA (4) in D_2O.

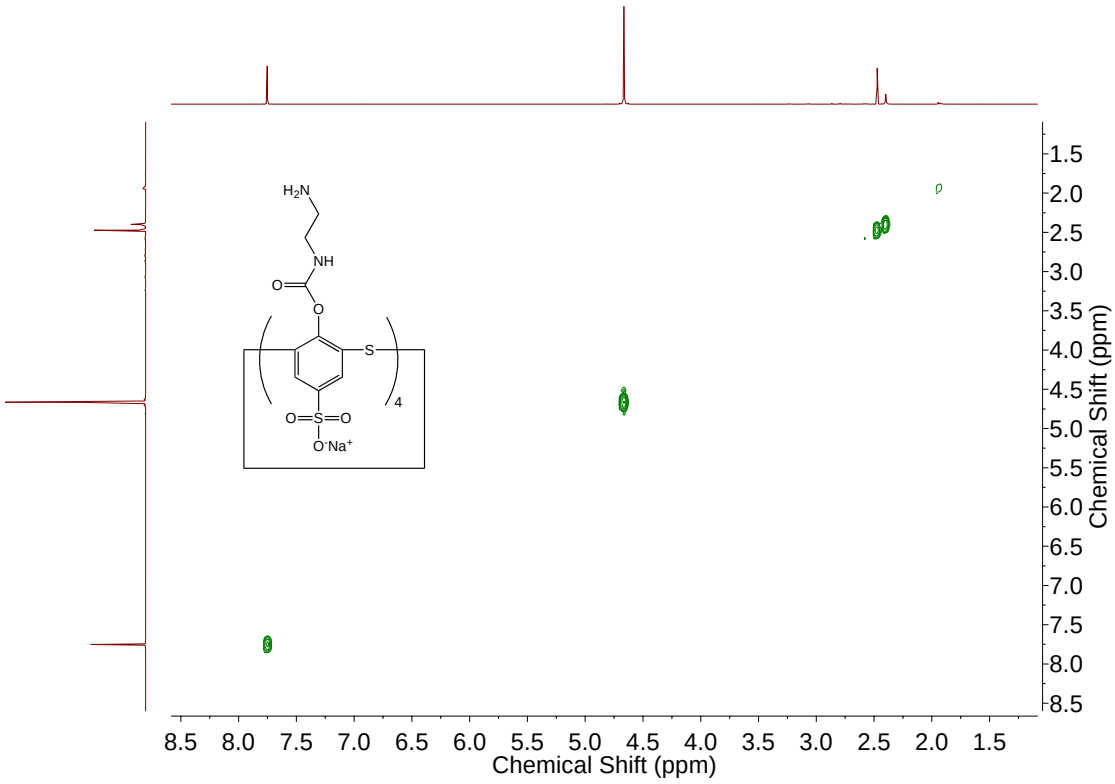

Supplementary Figure 20 | 2D ^{1}H-^{1}H COSY NMR spectrum of SC[4]AA (4) in D_2O.

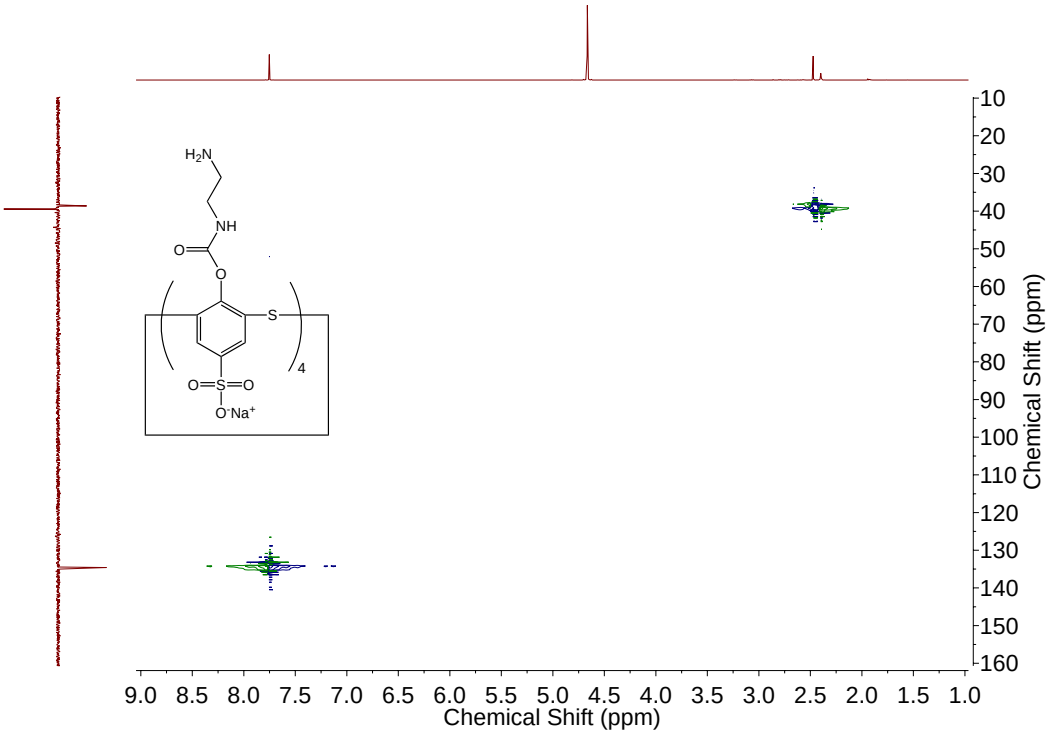

Supplementary Figure 21 | 2D ^{1}H-^{13}C HSQC NMR spectrum of SC[4]AA (4) in D_2O.

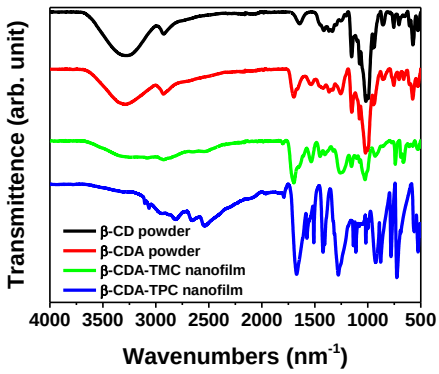

Supplementary Figure 22 | Fourier-transform infrared (FT-IR) spectra of the precursors, amino derivatives, and the resulting nanofilms. These include unfunctionalised *β*-cyclodextrin (*β*-CD) powder, synthesized amino-functionalised *β*-cyclodextrin (*β*-CDA) powder, and resulting nanofilms (*β*-CDA-TMC, and *β*-CDA-TPC) made from 0.1 wt.% *β*-CDA with 0.1 wt.% trimesoyl chloride (TMC) and 0.1 wt.% terephthaloyl chloride (TPC) respectively.

Supplementary Table 1. Functional groups analysed from FT-IR for unfunctionalised *β*-cyclodextrin (*β*-CD) powder, amino-functionalised *β*-cyclodextrin (*β*-CDA) powder, *β*-CDA-TMC nanofilm, and *β*-CDA-TPC nanofilm.

Wavenumbers (cm^{-1}) –functional group	*β*-CD powder	*β*-CDA powder	*β*-CDA-TMC nanofilm	*β*-CDA-TPC nanofilm
3290-(O-H) alcohol	√	√	√	√
2930-(C-H) alkane	√	√	√	√
1800-(C=O) carboxylic acid	×	×	√	√
1700-(C=O) amide	×	√	√	√
1610-(C=C) conjugated alkene	×	×	√	√
1530-(C-N) amide	×	√	√	√
1020-(C-O-C) ether	√	√	√	√

√ indicates the presence of the functional group. × indicates the absence of the functional group.

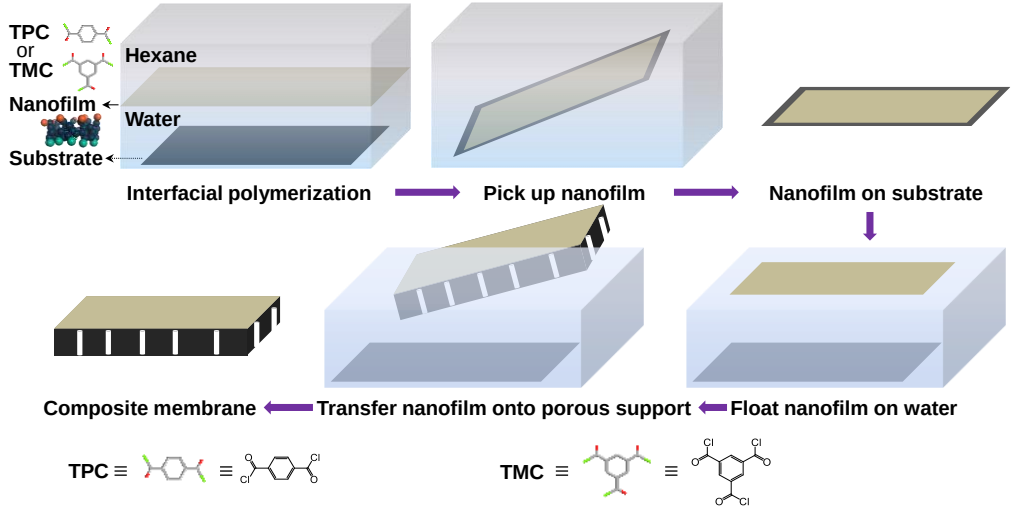

Supplementary Figure 23 | Schematic of interfacial polymerisation at a free interface. The reaction occurs between an aqueous phase containing amino-functionalised macrocycles and hexane phase containing terephthaloyl chloride (TPC) or trimesoyl chloride (TMC).

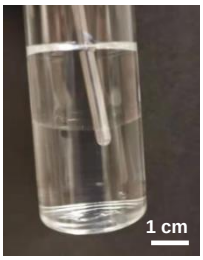

Supplementary Figure 24 | Photograph of the free interface between an aqueous phase containing unfunctionalised *β*-cyclodextrin and a hexane phase containing terephthaloyl chloride (TPC). No film was observed at the interface for this combination.

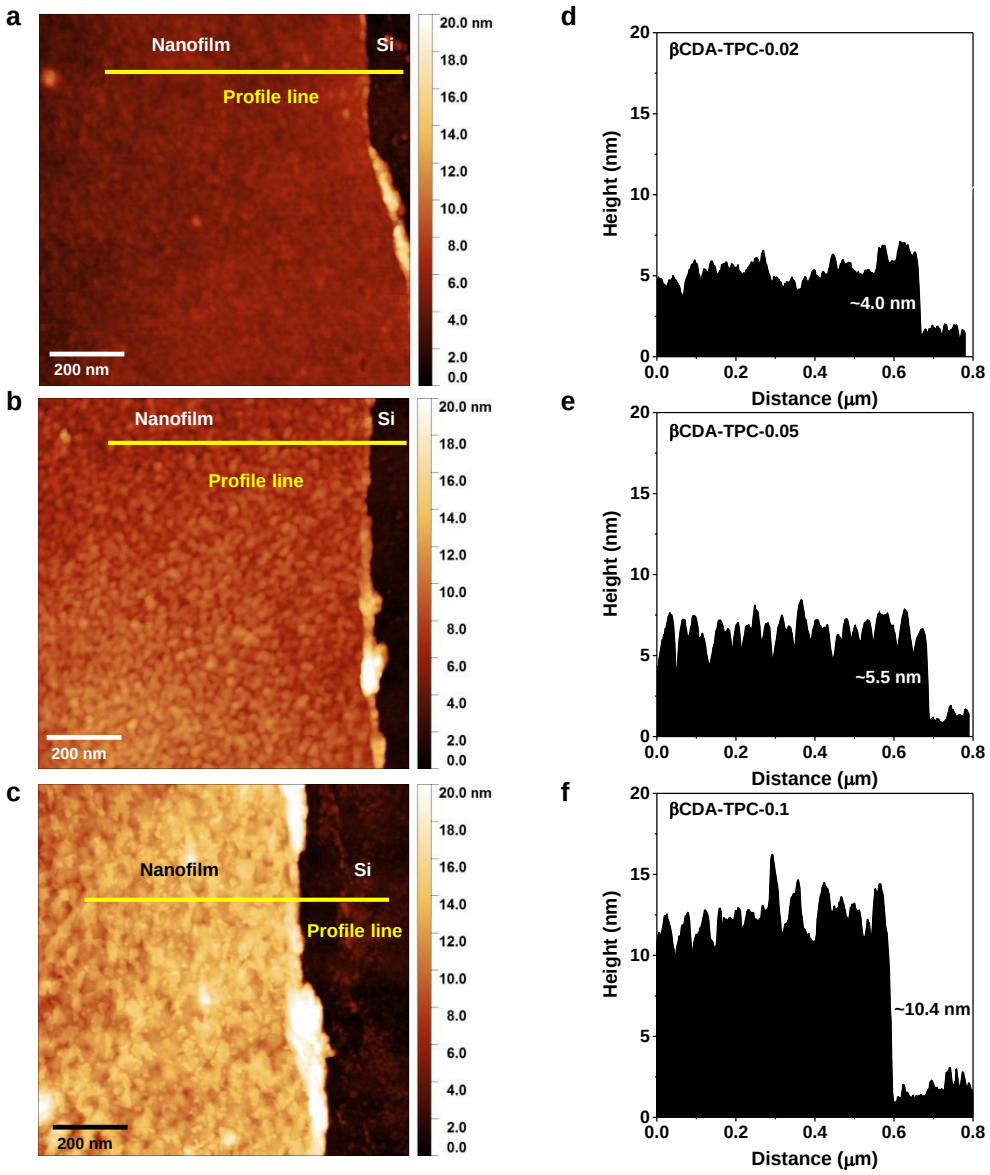

Supplementary Figure 25 | Atomic force microscopy (AFM) height images of the nanofilms. They were made from **a,** 0.02 wt.%, **b,** 0.05 wt.%, and **c,** 0.1 wt.% amino-functionalised *β*-cyclodextrin (*β*-CDA) and 0.1 wt.% terephthaloyl chloride (TPC) reacted for 1 min. **d-f,** Height along profile lines for respective nanofilms. The nanofilms were fabricated at the free interface and transferred onto silicon (Si) wafers.

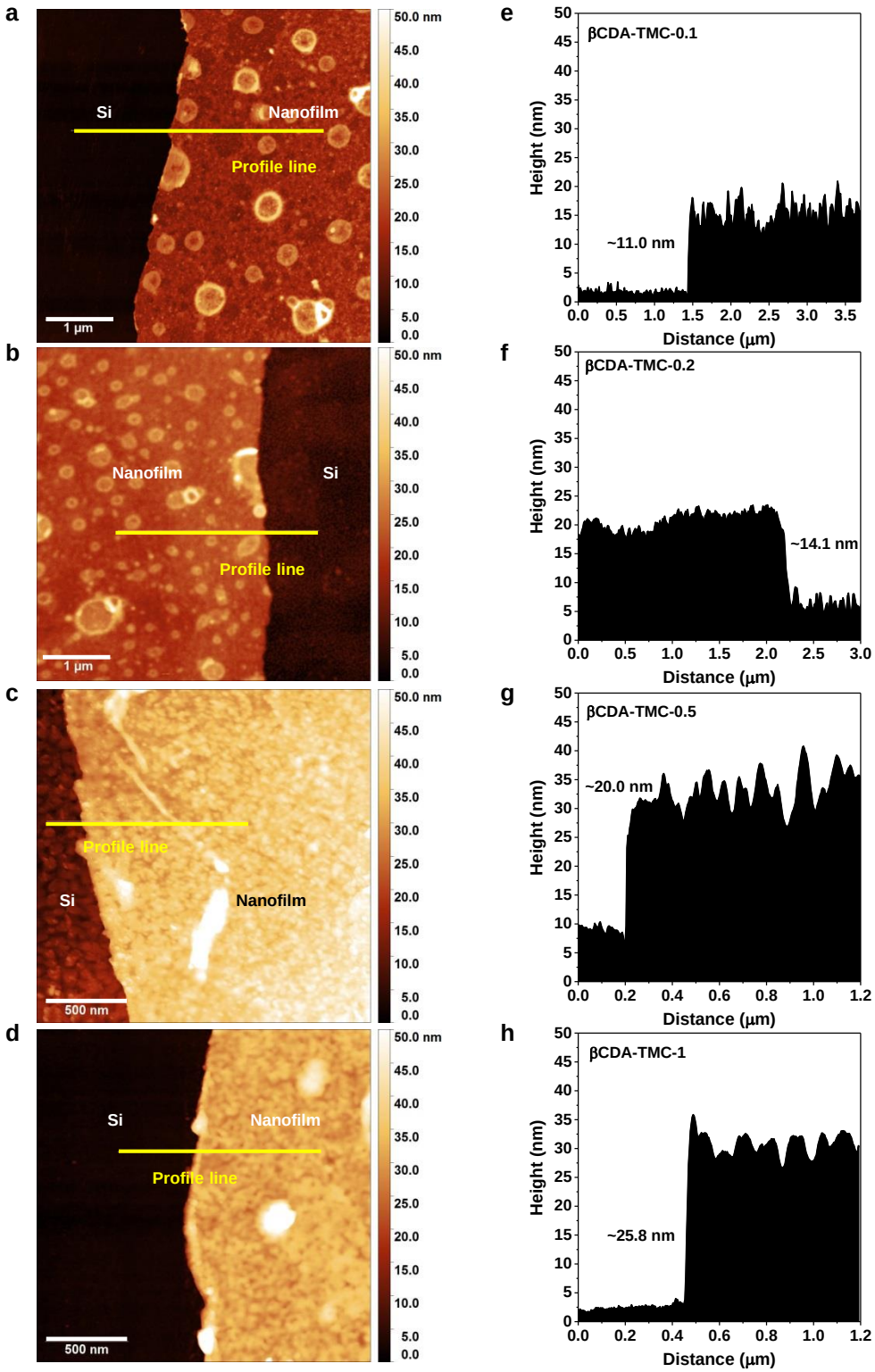

Supplementary Figure 26 | AFM height image of the nanofilms. They were made from **a,** 0.1 wt.%, **b,** 0.2 wt.%, **c,** 0.5 wt.%, and **d,** 1.0 wt.% amino-functionalised *β*-CDA and 0.1 wt.% trimesoyl chloride (TMC) reacted for 1 min. **e-h,** Height along profile lines scanned for respective nanofilms.

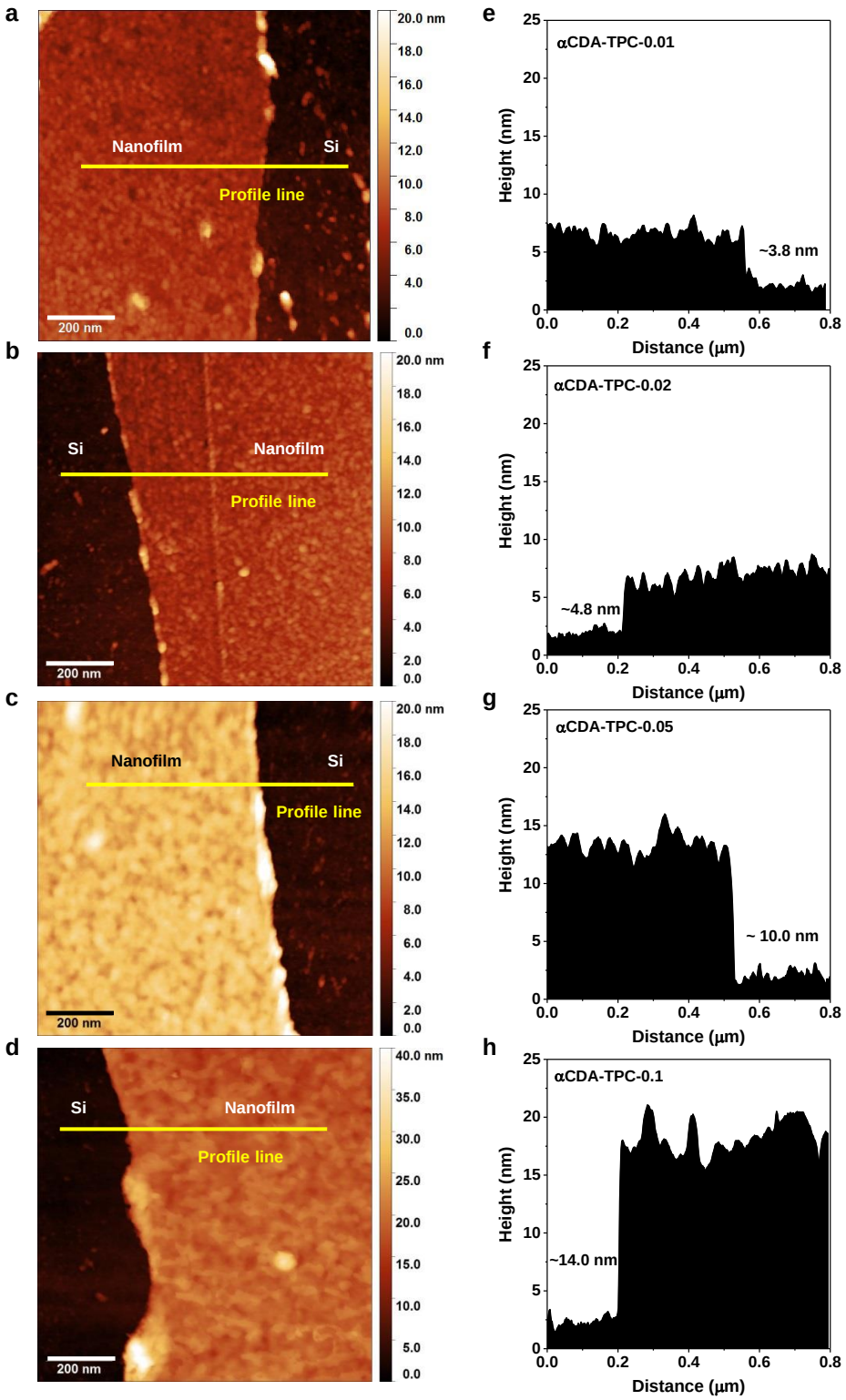

Supplementary Figure 27 | AFM height image of the nanofilms. They were made from **a,** 0.01 wt.%, **b,** 0.02 wt.%, **c,** 0.05 wt.%, **d,** 0.1 wt.% amino-functionalised α-cyclodextrin (α-CDA) and 0.1 wt.% TPC reacted for 1 min. **e-h,** Height along profile lines scanned for respective nanofilms.

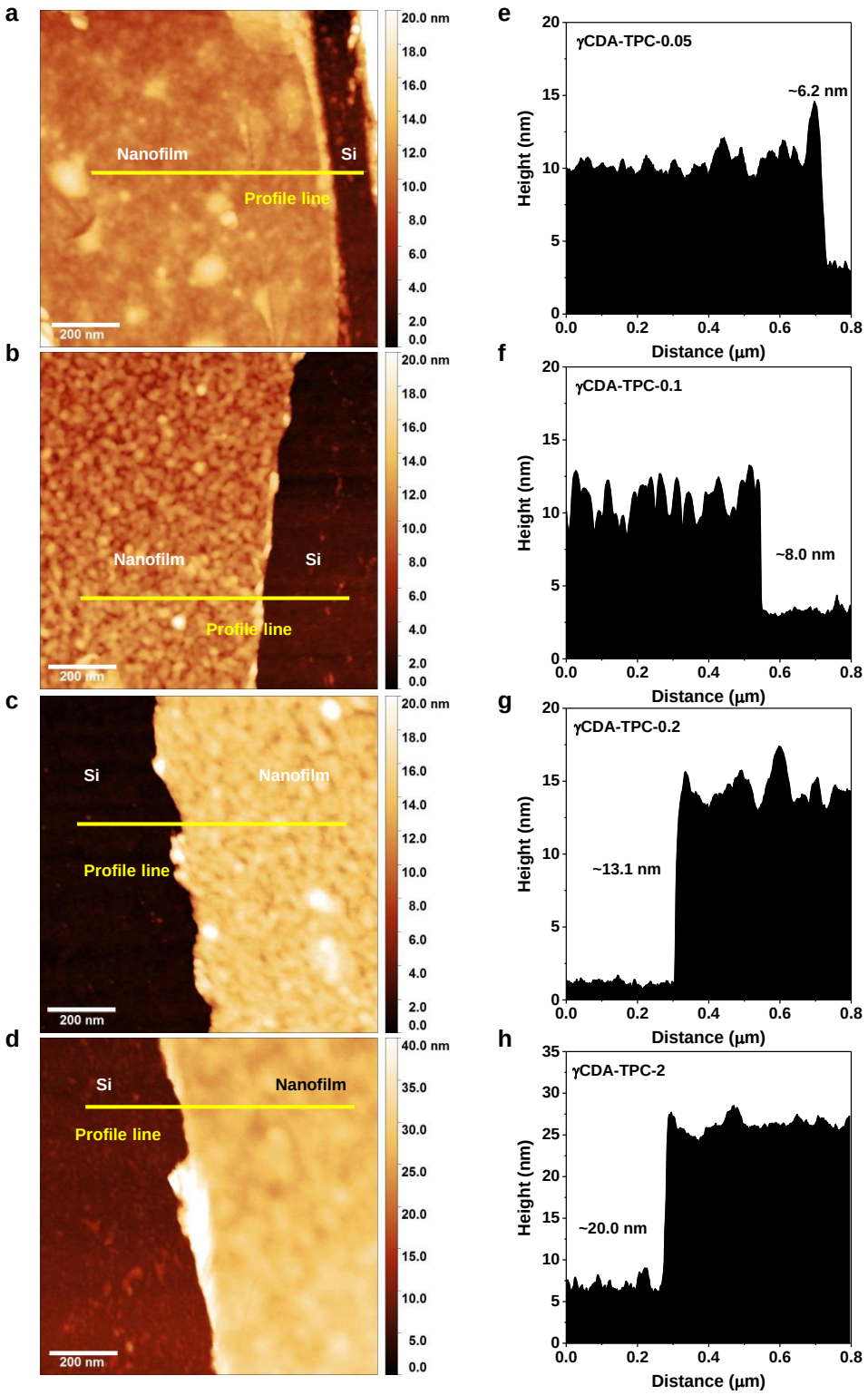

Supplementary Figure 28 | AFM height image of the nanofilms. They were made from **a,** 0.05 wt.%, **b,** 0.1 wt.%, **c,** 0.2 wt.%, and **d,** 2 wt.% amino-functionalised γ-cyclodextrin (γ-CDA) and 0.1 wt.% TPC reacted for 1 min. **e-h,** Height along profile lines scanned for respective nanofilms.

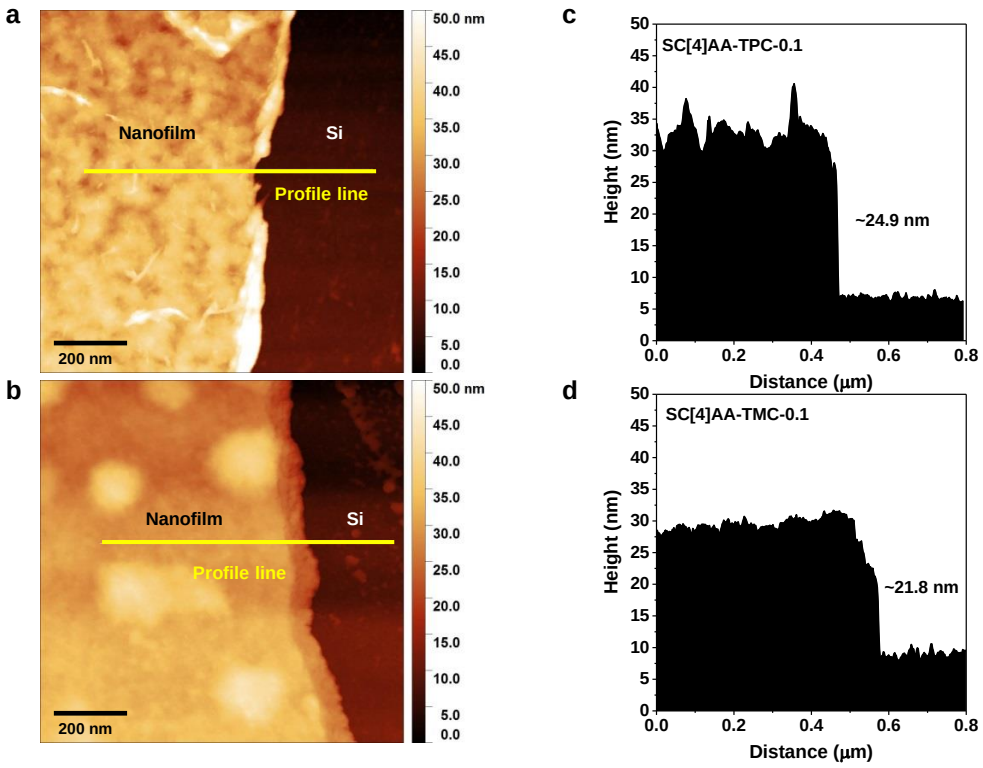

Supplementary Figure 29 | AFM height image of the nanofilms. They were made from 0.1 wt.% amino-functionalised 4-sulfocalix[4]arene (SC[4]AA) with **a,** 0.1 wt.% TPC and **b,** 0.1 wt.% TMC reacted for 20 min. **c** and **d,** Height along profile lines scanned for respective nanofilms. The nanofilm thicknesses were one order of magnitude thinner than those fabricated from unfunctionalised precursors[41].

Supplementary Table 2. Upper (narrow) and lower (wide) rim dimensions of macrocycles.

Property	***α*-CDA***	***β*-CDA***	**γ-CDA***	**SC[4]AA†**
Upper rim diameter (nm)	0.45	0.61	0.77	0.57
Lower rim diameter (nm)	0.57	0.78	0.95	0.57

*Dimensions adapted from the reported literature[42]. †Dimensions from molecular simulation, please refer to Supplementary Figure 48.

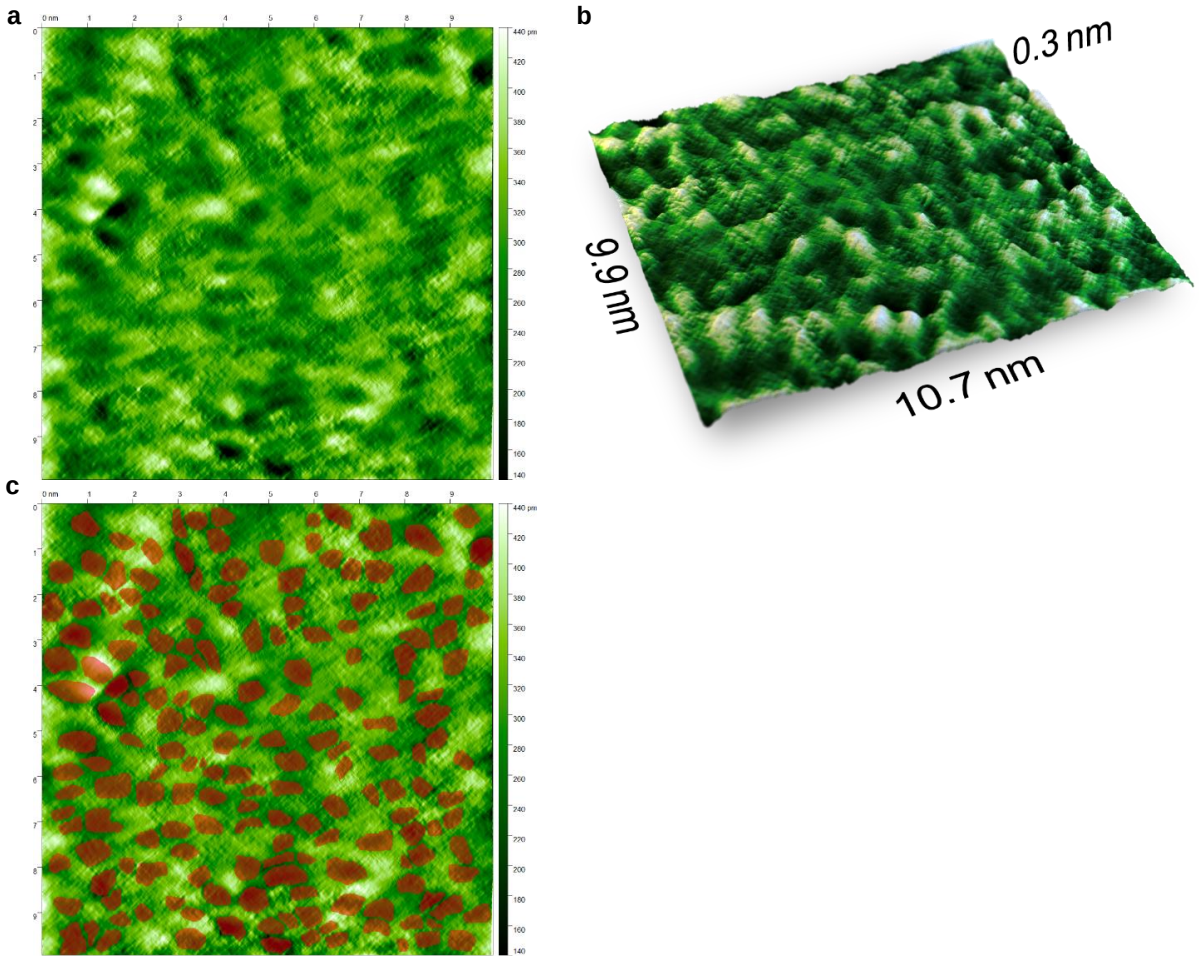

Supplementary Figure 30 | UHV AFM height images of nanofilms made from medium cavity *β*-CDA. Original **a,** 2D, **b,** 3D images, and **c,** 2D image with pores being marked.

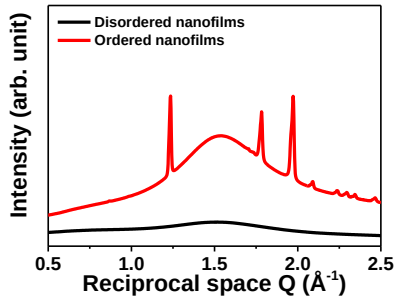

Supplementary Figure 31 | Powder X-ray diffraction of the nanofilm powders. They were made from disordered nanofilms (*β*-CDA-TMC-0.1) and ordered nanofilms (*β*-CDA-TPC-0.1).

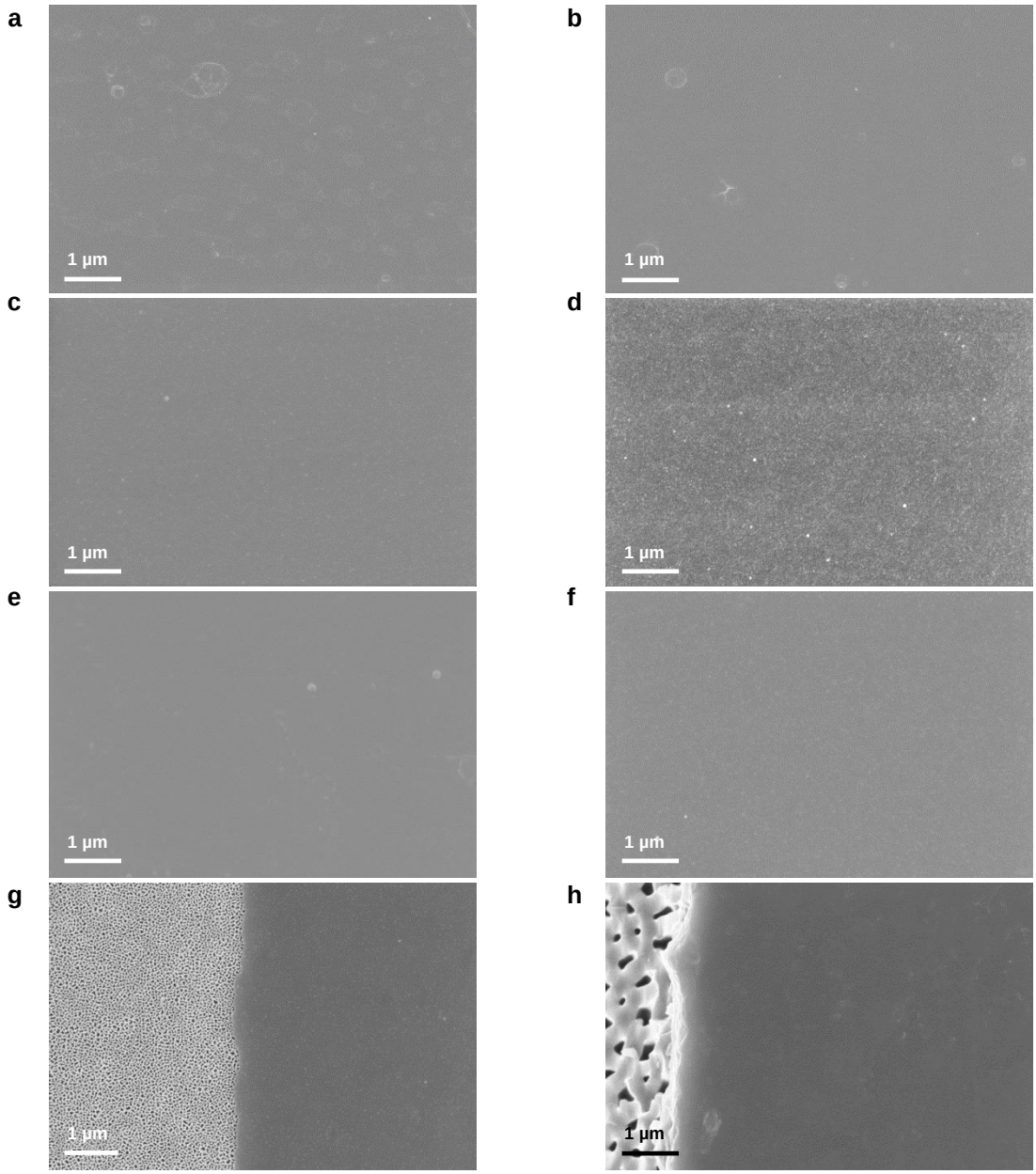

Supplementary Figure 32 | SEM surface images of the nanofilms. These include nanofilms (*β*-CDA-TMC-0.1) made from 0.1 wt.% amino-functionalised *β*-cyclodextrin (*β*-CDA) and 0.1 wt.% TMC revealing **a,** the front-surface-up and **b,** the back-surface-up transferred onto PAN supports. SEM images of the nanofilms (*β*-CDA-TPC-0.1) made from 0.1 wt.% *β*-CDA and 0.1 wt.% TPC revealing **c,** the front-surface-up and **d,** the back-surface-up transferred onto PAN supports. SEM images of **e,** the nanofilm (*β*-CDA-TMC-0.05) made from 0.05 wt.% *β*-CDA and 0.1 wt.% TMC and **f,** the nanofilm (*β*-CDA-TPC-0.05) made from 0.05 wt.% *β*-CDA and 0.1 wt.% TPC transferred onto PAN supports. SEM surface images of **g,** the nanofilm (*β*-CDA-TPC-0.1) made from 0.1 wt.% *β*-CDA and 0.1 wt.% TPC and **h,** the nanofilm (*α*-CDA-TPC-0.1) made from 0.1 wt.% *α*-CDA and 0.1 wt.% TPC transferred onto alumina supports.

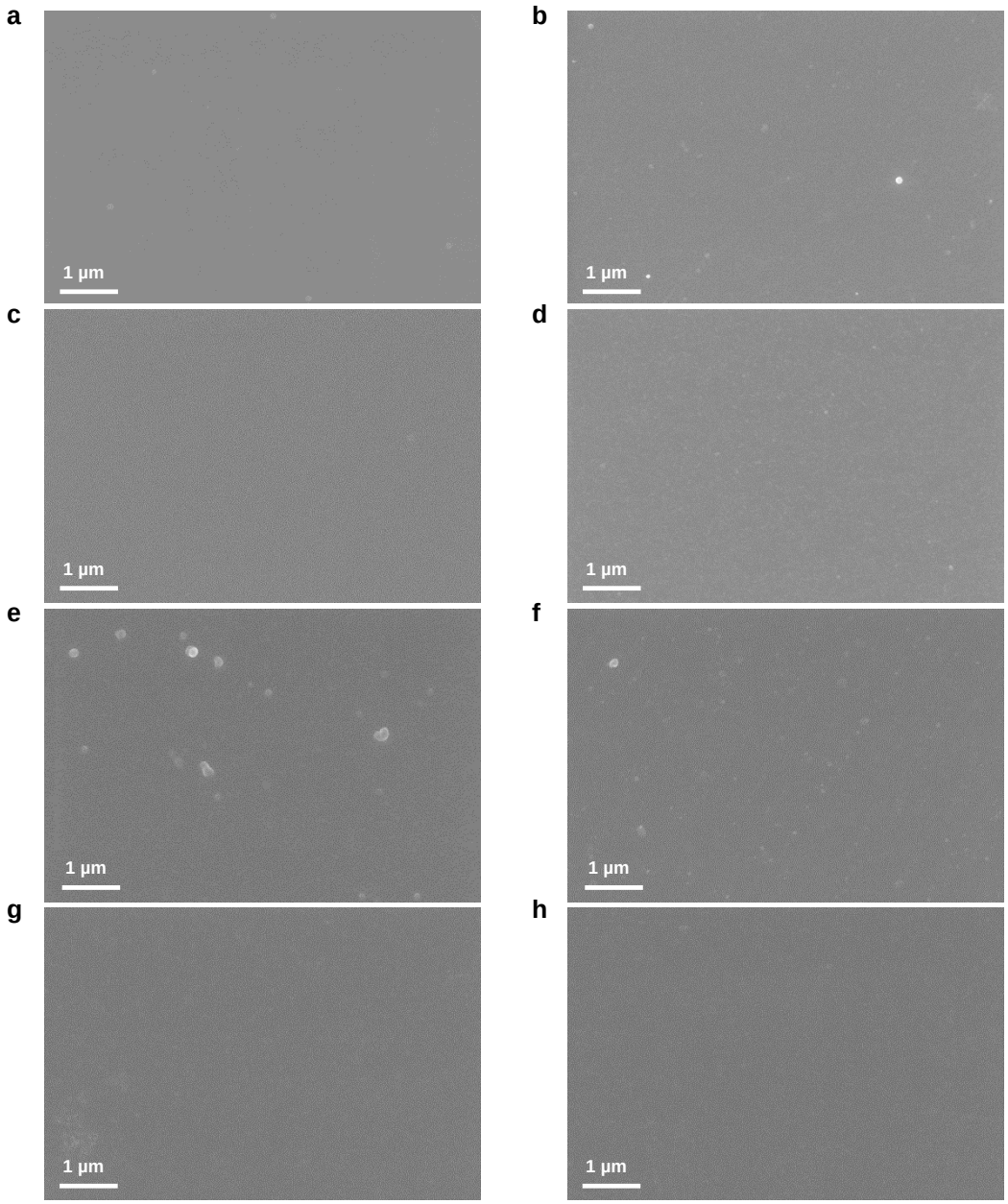

Supplementary Figure 33 | SEM surface images of the nanofilms. These include nanofilms made from **a,** 0.05 wt.% α-CDA (α-CDA-TPC-0.05), **b,** 0.1 wt.% α-CDA (α-CDA-TPC-0.1), **c,** 0.05 wt.% γ-CDA (γ-CDA-TPC-0.05), **d,** 0.1 wt.% γ-CDA (γ-CDA-TPC-0.1), **e,** 0.2 wt.% γ-CDA (γ-CDA-TPC-0.2), and **f,** 2 wt.% γ-CDA (γ-CDA-TPC-2) with 0.1 wt.% terephthaloyl chloride (TPC) reacted for 1 min and transferred onto PAN supports. SEM images of **g,** the nanofilms (SC[4]AA-TPC-0.1) made from 0.1 wt.% amino-functionalised 4-sulfocalix[4]arene (SC[4]AA) reacted with 0.1 wt.% TPC and **h,** the nanofilms (SC[4]AA-TMC-0.1) made from 0.1 wt.% SC[4]AA reacted with 0.1 wt.% TMC for 20 min and transferred onto PAN supports.

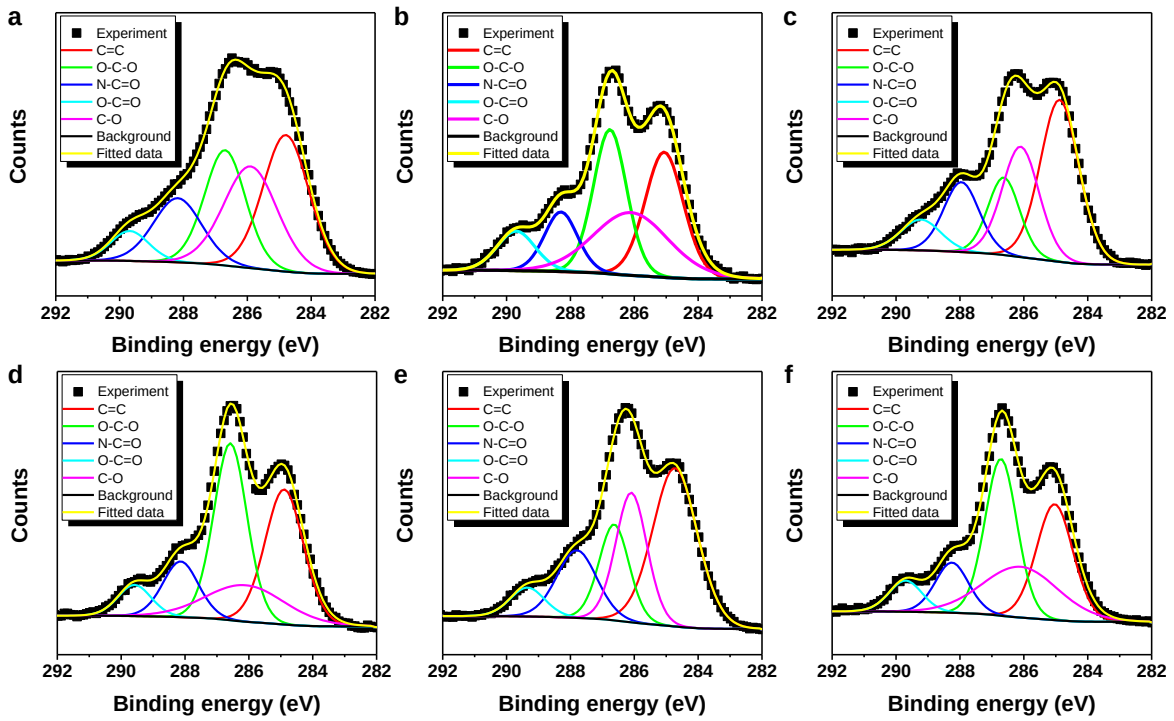

Supplementary Figure 34 | X-ray photoelectron spectroscopy (XPS) C1s spectrum of the nanofilms. They were made from **a,** 0.1 wt.% amino-functionalised *α*-cyclodextrin (*α*-CDA) and terephthaloyl chloride (TPC) (*α*-CDA-TPC-0.1), **b,** 0.1 wt.% *β*-CDA and TPC (*β*-CDA-TPC-0.1), **c,** 0.1 wt.% *β*-CDA and trimesoyl chloride (TMC) (*β*-CDA-TMC-0.1), **d,** 0.1 wt.% *γ*-CDA and TPC (*γ*-CDA-TPC-0.1), **e,** 0.2 wt.% *γ*-CDA and TPC (*γ*-CDA-TPC-0.2), and **f,** 2 wt.% *γ*-CDA and TPC (*γ*-CDA-TPC-2). Concentration of acyl chloride for all nanofilms were controlled at 0.1 wt.%.

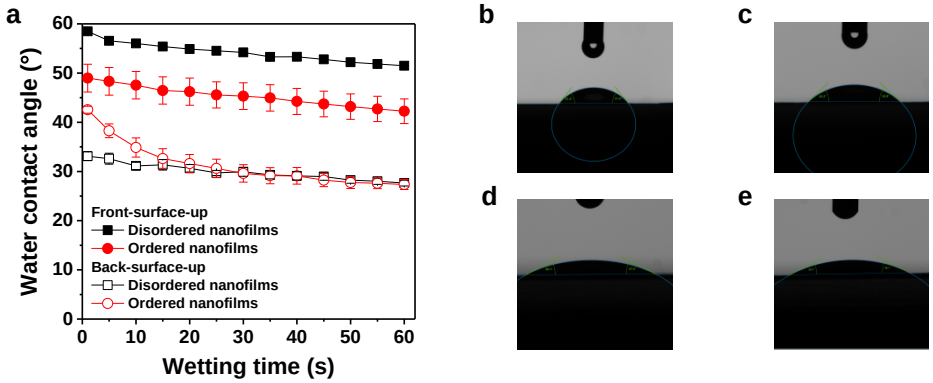

Supplementary Figure 35 | Water contact angle of disordered nanofilms (*β*-CDA-TMC-0.1) and ordered nanofilms (*β*-CDA-TPC-0.1) with their front or back surfaces facing up. a, Measurement of water contact angle over wetting time of 60 sec. Photographs of water droplets on the surface of **b,** disordered nanofilms and **c,** ordered nanofilms with front-surface-up, and **d,** disordered nanofilms and **e,** ordered nanofilms with back-surface-up. High water contact angle reveals a more hydrophobic surface that creates potential for fast transport of non-polar solvent.

Supplementary Table 3. Properties of dye molecules used for OSN. Charge 0 denotes neutral charge, - denotes negative charge, and + denotes positive charge.

Dye molecule name	Structure	Dimension (nm × nm)	Molecular weight (g mol^{-1})	Charge
4-nitrophenol (4NP)		0.25 × 0.63	139	0
Azobenzene (AZB)		0.43 × 0.90	182	0
Methyl orange (MO)	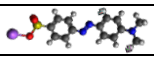	0.51 × 1.5	327	-
Safranin O (SO)		0.73 × 0.97	351	+
Congo red (CR)	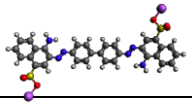	0.89 × 2.4	696	-
Sunset yellow (SY)	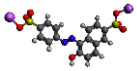	1.1 × 1.7	452	-
Acid fuchsin (ACF)	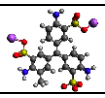	1.2 × 1.3	585	-
Brilliant blue R (BB)	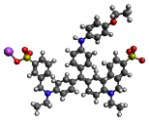	1.4 × 2.1	826	-

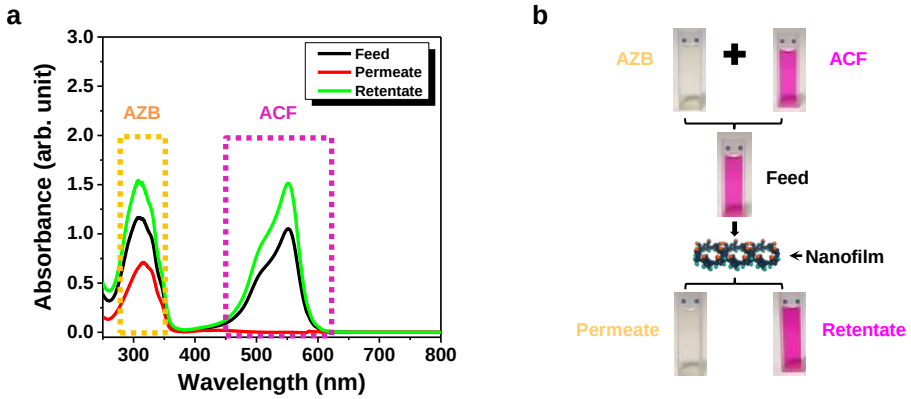

Supplementary Figure 36 | Rejection of a feed mixture containing azobenzene (AZB) and acid fuchsin (ACF) in methanol through β-CDA-TPC-0.1 membrane. a, UV-vis spectra and **b,** photos of the feed, permeate, and retentate.

Supplementary Table 4. Solubility parameter and viscosity of various solvents.

Solvent	Solubility parameter, δ, (MPa$^{0.5}$)*	Viscosity, μ, (10^{-3} Pa.s)*
Water	48.0	0.89
Acetonitrile	24.6	0.32
Methanol	29.7	0.49
Acetone	20.1	0.316
Hexane	14.4	0.297
Heptane	15.3	0.33
Toluene	18.2	0.52

*The values were adapted from the literature[2,43].

Supplementary Table 5. Performance of commercial polyamide-based nanofiltration membranes and composite membranes comprising nanofilms made from amino-functionalised macrocycles and acyl chloride at a free interface.

Membrane (macrocycle-acyl chloride-wt.%-remark)	Pure methanol permeance ($L\ m^{-2}\ h^{-1}\ bar^{-1}$)	Dye rejection (%)							
		4NP (0.25 nm)	AZB (0.43 nm)	MO (0.51 nm)	SO (0.73 nm)	CR (0.89 nm)	SY (1.1 nm)	ACF (1.2 nm)	BB (1.4 nm)
α-CDA-TPC-0.05	7.64 ± 0.1	18.0 ± 1.0	33.9 ± 0.9	93.0 ± 1.2	94.0 ± 0.9	98.6 ± 0.3	97.2 ± 0.6	99.4 ± 0.2	99.3 ± 0.3
α-CDA-TPC-0.1	5.75 ± 0.2	8.4 ± 2.5	36.2 ± 4.9	90.3 ± 0.5	95.8 ± 0.8	99.3 ± 0.1	99.0 ± 0.1	99.5 ± 0.4	99.3 ± 0.3
α-CDA-TPC-0.1-Al*	9.51 ± 0.3	9.8 ± 1.5	18.3 ± 3.4	91.3 ± 1.2	96.3 ± 2.0	99.6 ± 0.2	96.0 ± 1.2	97.3 ± 1.4	99.7 ± 0.1
β-CDA-TPC-0.05	9.84 ± 0.2	4.7 ± 0.7	28.3 ± 2.3	81.3 ± 5.2	95.5 ± 1.2	98.3 ± 0.3	98.3 ± 0.5	99.8 ± 0.1	99.6 ± 0.1
β-CDA-TPC-0.1	6.26 ± 0.4	10.6 ± 0.3	27.7 ± 0.3	75.1 ± 3.9	96.2 ± 0.8	98.6 ± 0.4	96.0 ± 0.3	99.4 ± 0.3	99.8 ± 0.1
β-CDA-TPC-0.1-back†	10.4 ± 0.8	9.2 ± 1.7	23.8 ± 2.5	72.0 ± 4.0	90.7 ± 1.3	98.8 ± 0.5	94.4 ± 2.3	99.0 ± 0.3	98.5 ± 0.5
β-CDA-TPC-0.1-Al*	11.9 ± 0.4	15.6 ± 0.8	26.4 ± 1.6	83.2 ± 5.3	96.5 ± 2.1	98.3 ± 1.2	96.0 ± 1.7	99.7 ± 0.1	99.5 ± 0.1
β-CDA-TPC-2-direct‡	1.14 ± 0.1	42.1 ± 2.7	63.6 ± 3.1	92.6 ± 2.4	94.7 ± 3.3	99.0 ± 0.3	98.5 ± 0.7	98.0 ± 0.8	99.1 ± 0.2
β-CDA-TMC-0.05	3.91 ± 0.1	6.5 ± 0.5	26.9 ± 2.1	92.4 ± 1.6	92.2 ± 1.2	98.4 ± 0.3	95.8 ± 0.9	98.2 ± 0.5	98.5 ± 0.6
β-CDA-TMC-0.1	3.00 ± 0.5	10.0 ± 0.7	16.5 ± 2.1	93.0 ± 1.5	98.0 ± 0.4	99.8 ± 0.1	97.2 ± 0.7	99.2 ± 0.2	99.7 ± 0.1
β-CDA-TMC-0.1-back†	6.27 ± 0.3	23.2 ± 3.2	44.5 ± 2.0	93.6 ± 1.3	93.4 ± 1.6	98.9 ± 0.3	98.0 ± 0.4	99.0 ± 0.1	99.5 ± 0.1
γ-CDA-TPC-0.05	9.87 ± 0.2	3.6 ± 1.1	12.3 ± 0.2	57.0 ± 5.3	58.2 ± 6.1	99.0 ± 0.1	91.1 ± 0.8	98.0 ± 0.3	99.2 ± 0.2
γ-CDA-TPC-0.1	9.30 ± 0.5	7.4 ± 0.8	23.5 ± 4.4	60.0 ± 3.6	75.7 ± 2.1	98.6 ± 1.0	94.5 ± 1.6	99.7 ± 0.1	99.8 ± 0.1
γ-CDA-TPC-0.2	1.92 ± 0.3	15.2 ± 1.0	58.9 ± 0.8	91.2 ± 3.7	94.6 ± 4.6	99.1 ± 0.2	96.7 ± 1.8	99 ± 0.1	99.8 ± 0.1
γ-CDA-TPC-2	1.61 ± 0.2	40.5 ± 2.0	70.2 ± 3.5	96.7 ± 1.2	98.6 ± 1.0	99.0 ± 0.1	99.7 ± 0.1	99.7 ± 0.2	99.9 ± 0.1
SC[4]AA-TPC-0.1‡	3.08 ± 0.4	25.3 ± 1.0	48.2 ± 2.3	84.3 ± 2.7	92.6 ± 0.8	94.3 ± 1.0	92.9 ± 0.9	94.2 ± 2.1	98.1 ± 0.7
SC[4]AA-TMC-0.1‡	2.51 ± 0.2	22.7 ± 0.8	52.6 ± 1.9	95.7 ± 1.3	98.6 ± 0.4	99.6 ± 0.2	99.3 ± 0.1	99.6 ± 0.1	99.8 ± 0.1
TriSep™ TS40⁂	8.65 ± 3.0	41.2 ± 1.7	48.0 ± 1.4	85.4 ± 4.9	48.7 ± 1.8	83.5 ± 13.5	90.9 ± 8.2	42.7 ± 12.8	45.1 ± 16.6
Suez™ (GE) DK⁂	4.96 ± 0.5	38.2 ± 0.6	49.4 ± 6.4	93.3 ± 0.6	88.6 ± 1.2	98.9 ± 0.6	97.6 ± 0.5	75.8 ± 8.4	60.3 ± 29.6
Synder Filtration™ NDX⁂	2.55 ± 0.3	49.4 ± 3.4	71.9 ± 5.0	96.3 ± 2.4	97.6 ± 0.7	98.6 ± 1.4	97.8 ± 2.1	95.7 ± 1.7	97.5 ± 0.5

Unless specified otherwise, nanofilms were made from amino-functionalised macrocycles and acyl chloride via interfacial polymerisation at a free interface reacted for 1 min and then transferred with the front surface facing up onto PAN supports to form composite membranes. *Nanofilms were transferred onto alumina supports to create composite membranes. †Nanofilms were flipped over and transferred with the back surface facing up (back-surface-up) onto the supports. ‡Nanofilms were directly made on PAN supports via conventional interfacial polymerization. ‡Nanofilms were fabricated via interfacial reaction for 20 min. ⁂Commercial polyamide-based nanofiltration membranes. All experiments were carried out in a dead-end filtration cell at a constant pressure 10 bar and a constant temperature 25 °C under constant stirring at 250 rpm. Dye concentrations were maintained at 20 mg L^{-1} throughout all experiments.

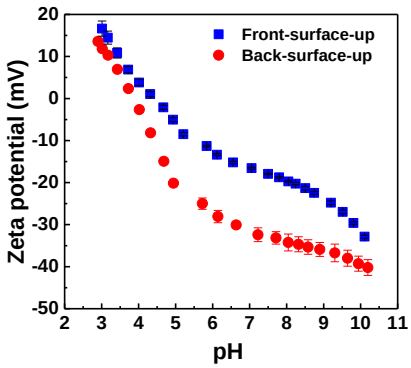

Supplementary Figure 37 | Zeta potential of the front and back surfaces of the *β*-CDA-TMC-0.1 nanofilm.

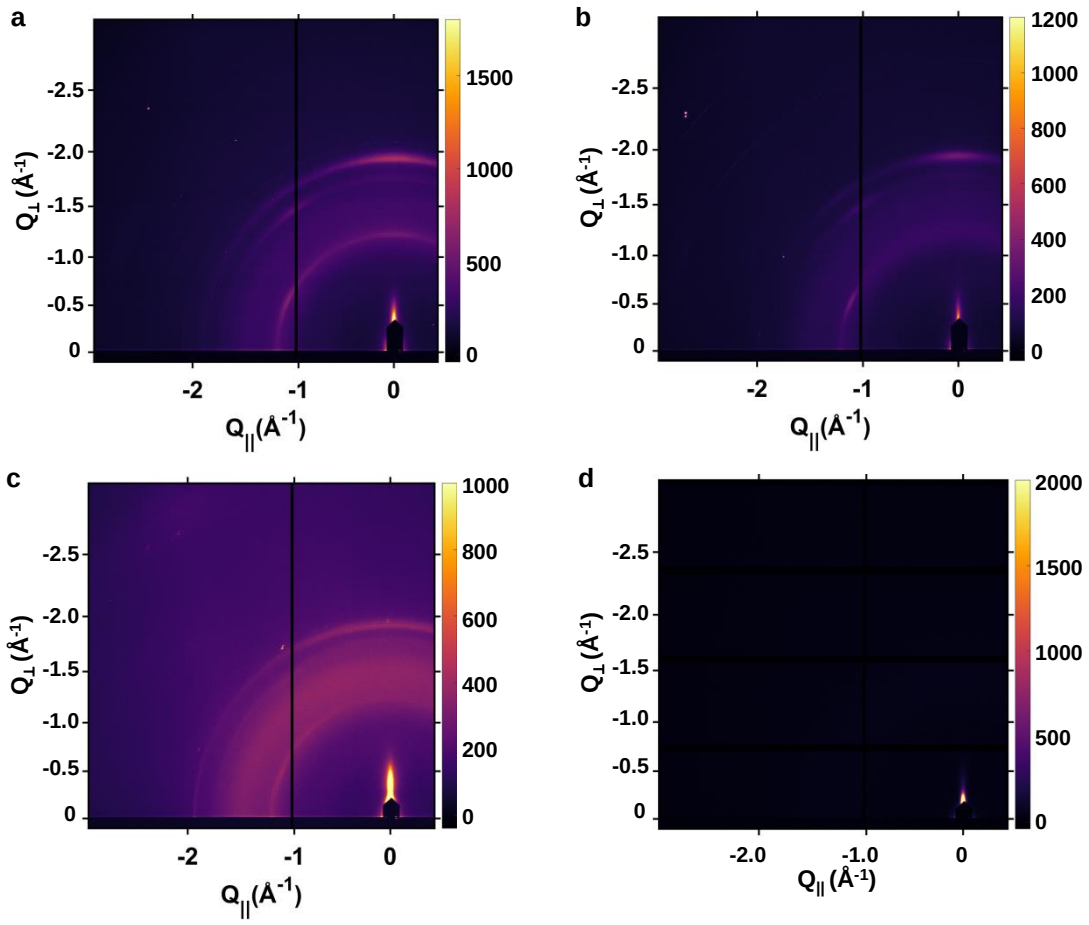

Supplementary Figure 38 | GI-WAXS images of the nanofilms. Two-dimensional images of nanofilms made from increasing *γ*-CDA concentrations **a,** 0.05 wt.% *γ*-CDA (*γ*-CDA-TPC-0.05), **b,** 0.1 wt.% *γ*-CDA (*γ*CDA-TPC-0.1), **c,** 0.2 wt.% *γ*-CDA (*γ*-CDA-TPC-0.2), and **d,** 2 wt.% *γ*-CDA (*γ*-CDA-TPC-2) with 0.1 wt.% terephthaloyl chloride (TPC). The corresponding one-dimensional image is shown in Fig. 3e in the main text.

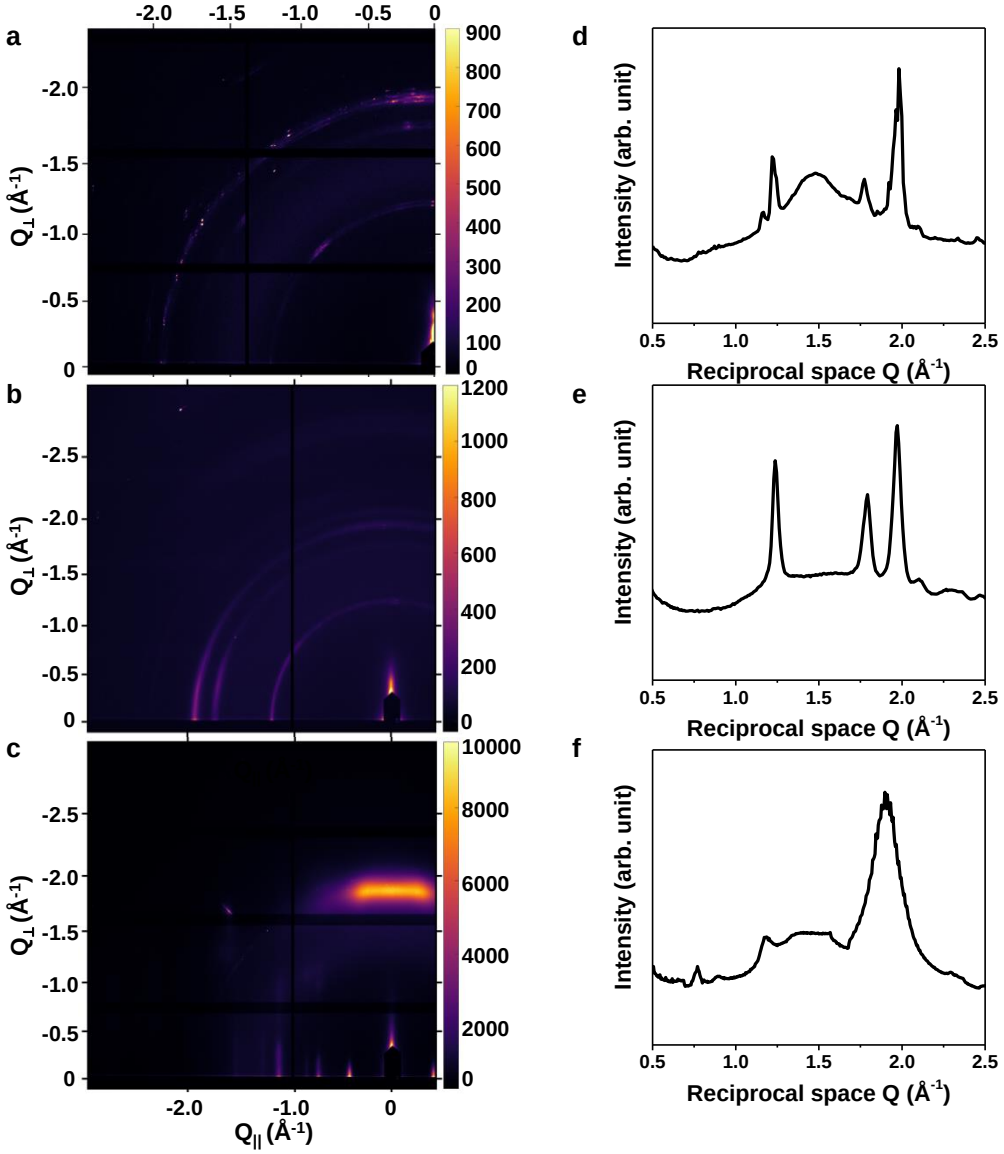

Supplementary Figure 39 | GI-WAXS images of the nanofilms. Two dimensional images of nanofilms made **a,** 0.01 wt.% *α*-CDA (*α*-CDA-TPC-0.01) and **b,** 0.01 wt.% *γ*-CDA (*γ*-CDA-TPC-0.01) with 0.1 wt.% TPC, and **c,** 0.01 wt.% *β*-CDA with 0.1 wt.% TMC (*β*-CDA-TMC-0.01). **d-f,** GI-WAXS one-dimensional images of the nanofilms in a-c respectively.

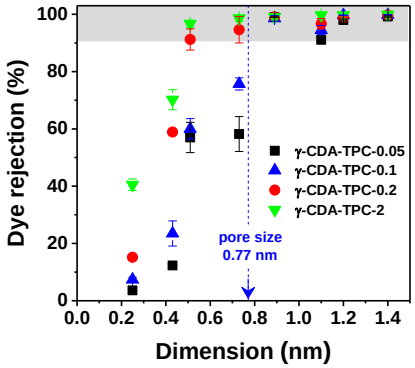

Supplementary Figure 40 | Dye rejections of the composite membranes. They comprise nanofilms made from various concentrations of γ-CDA with constant 0.1 wt.% TPC.

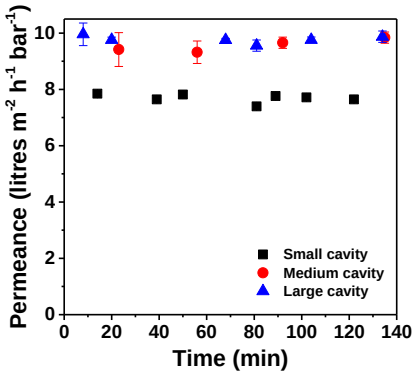

Supplementary Figure 41 | Pure methanol permeance of the composite membranes. They comprise nanofilms made from small cavity (α-CDA-TPC), medium cavity (β-CDA-TPC), and large cavity (γ-CDA-TPC) at constant concentrations of 0.05 wt.% CDA and 0.1 wt.% TPC reacted for 1 min, and transferred onto PAN supports.

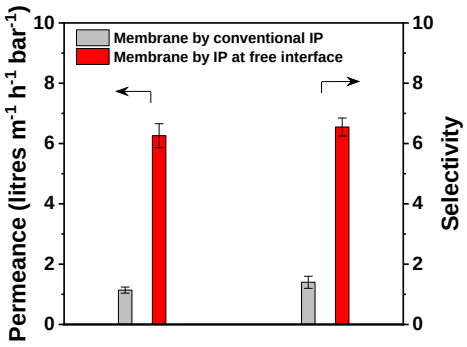

Supplementary Figure 42 | Comparison of performance for composite membranes. They comprise nanofilms made by conventional interfacial polymerisation (IP) directly on supports and by IP at free interface (β-CDA-TPC-0.1) and subsequently transferred onto supports. Selectivity of solute size 0.51 nm / 0.73 nm is plotted.

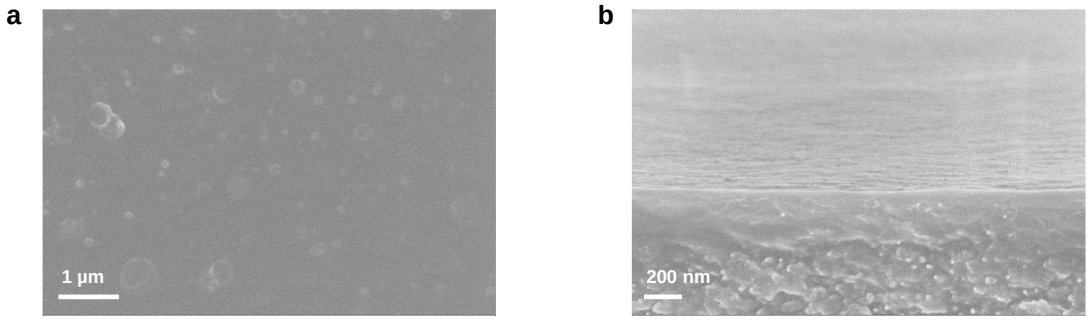

Supplementary Figure 43 | SEM images of composite membranes fabricated directly on supports by conventional interfacial polymerisation. a, surface, and **b,** cross sectional images.

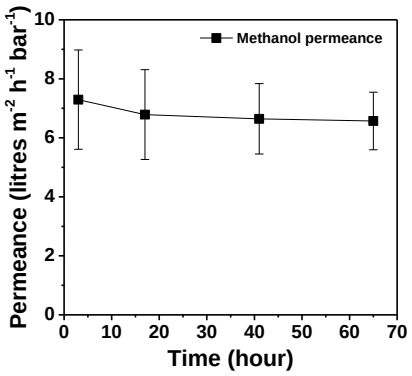

Supplementary Figure 44 | Long-term methanol permeance for the composite membranes. Membranes comprise nanofilms (*β*-CDA-TPC-0.1) made from 0.1 wt.% *β*-CDA and 0.1 wt.% TPC and then transferred onto PAN supports. The membranes were tested in a crossflow rig for 3 days at 25 °C under 10 bar with flowrate of 50 L h^{-1}.

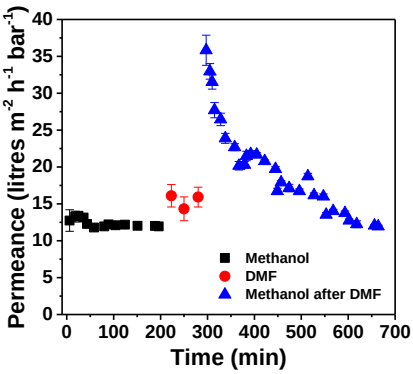

Supplementary Figure 45 | Impact of DMF post treatment. Methanol permeance before and after dimethylformamide (DMF) treatment for the composite membrane comprising nanofilms (*β*-CDA-TPC-0.1-Al) made from 0.1 wt.% *β*-CDA and 0.1 wt.% TPC and then transferred onto alumina supports. No activation by DMF was observed for the membrane.

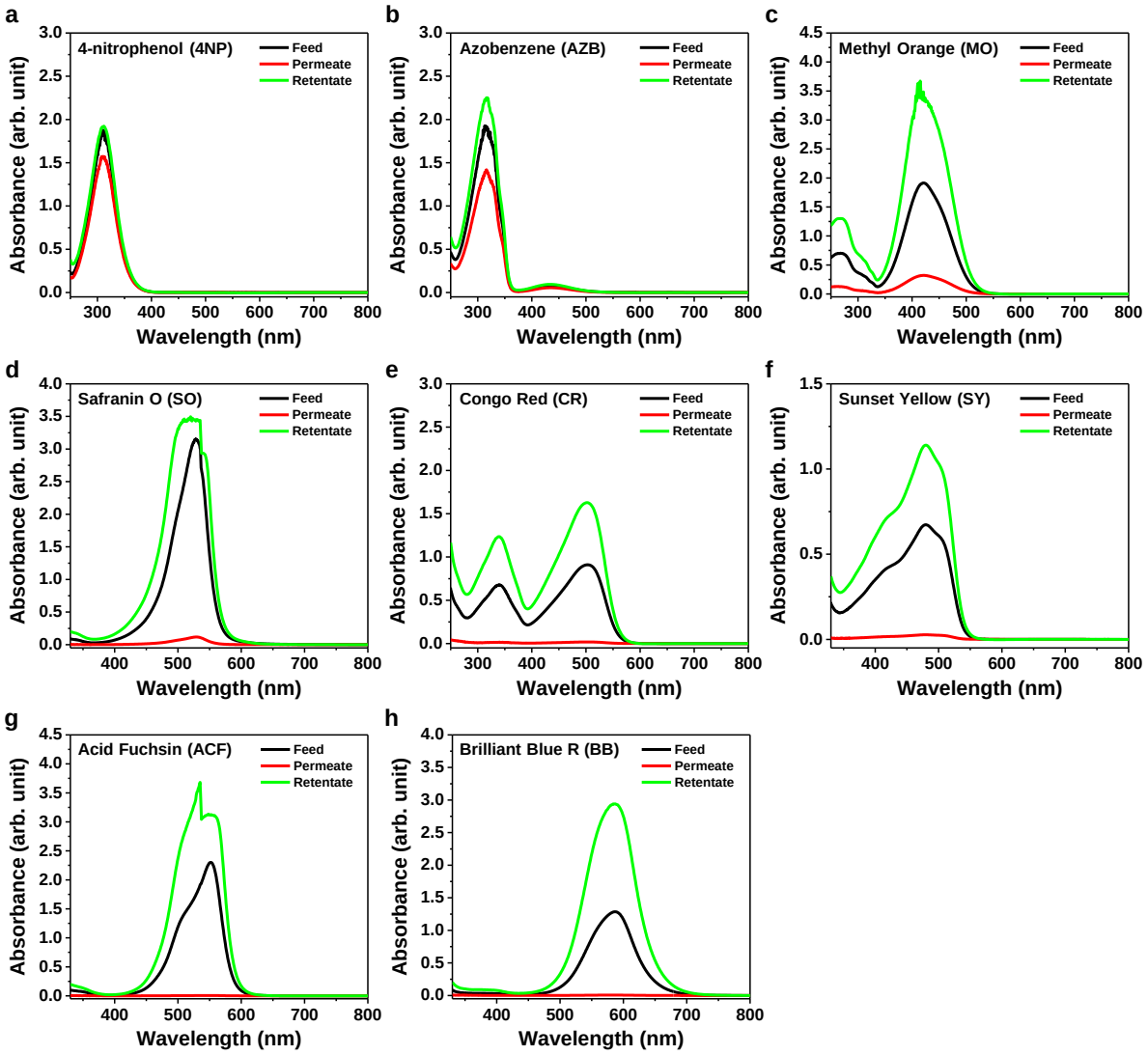

Supplementary Figure 46 | Typical ultraviolet-visible (UV-vis) absorption spectra of dyes in feed, permeate, and retentate demonstrating the rejection performance of composite membranes. This membrane comprised nanofilms (*β*-CDA-TPC-0.1-Al) made from 0.1 wt.% *β*-CDA and 0.1 wt.% terephthaloyl chloride (TPC) at the free interface for 1 min and then transferred onto alumina supports.

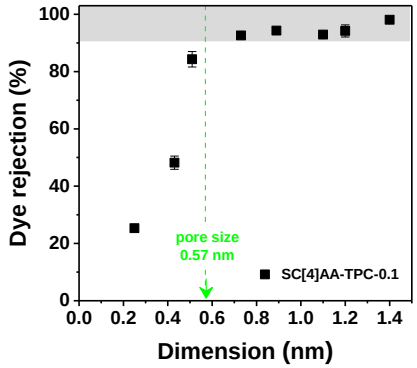

Supplementary Figure 47 | Dye rejections of the composite membranes. They comprise nanofilms made from amino-functionalised 4-sulfocalix[4]arene sodium salt (SC[4]AA) and 0.1 wt.% terephthaloyl chloride (TPC) at the free interface for 20 min and then transferred onto PAN supports.

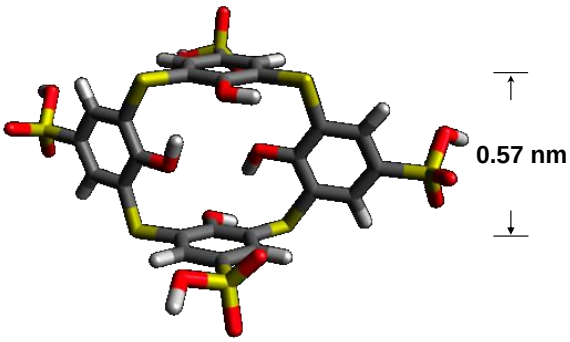

Supplementary Figure 48 | Schematic illustrating the molecular dimensions of amino-functionalised 4-sulfocalix[4]arene sodium salt (SC[4]AA).

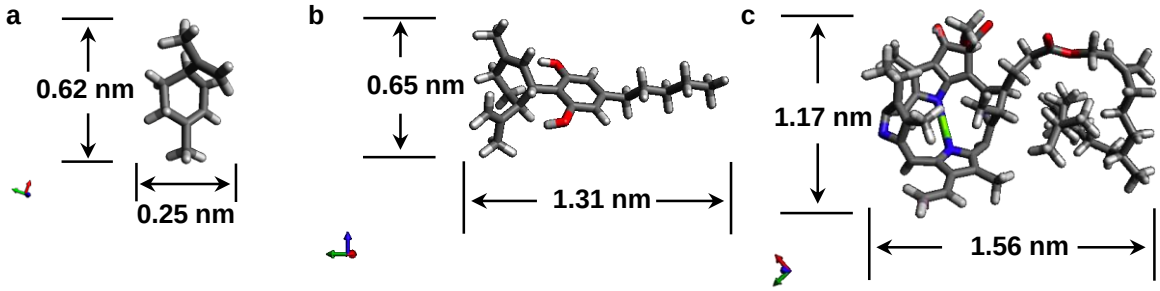

Supplementary Figure 49 | Schematic illustrating the molecular dimensions. a, limonene (136 g mol^{-1}), **b,** CBD (314 g mol^{-1}), and **c,** chlorophyll (893 g mol^{-1}).

Supplementary Table 6. Comparison of selectivity performance between membranes reported in literature and membranes fabricated from amino-functionalised macrocycles in this work.

Membrane material	Methanol permeance ($L\ m^{-2}\ h^{-1}\ bar^{-1}$)	MW <300 g mol^{-1}		MW 300-400 g mol^{-1}		MW 400-500 g mol^{-1}		Selectivity		Ref.
		Dye (MW)	Rejection (%)	Dye (MW)	Rejection (%)	Dye (MW)	Rejection (%)	MW<300 / MW 300-400	MW 300-400 / MW 400-500	
Cyclodextrin	4.9			MO (327)	67	IC (466)	88	-	2.75	8
Trianglamine macrocycle	22			MO (327)	83	OG (452)	96	-	4.25	9
COF	72	NR (229)	2	SO (351)	5	PR (453)	5	1.03	1.00	13
Cyclodextrin	17	MR (291)	60	MO (327)	88	RBB (442)	95	1.58	2.40	17
Polyarylate	8	CSG (249)	70	DR (314)	90	CV (408)	97	3.00	3.33	30
Graphene oxide	9	HNSA (246)	99.9	DR (314)	99.9	CV (408)	99.9	1.00	1.00	31
Polyimide	1.6			MO (327)	60	OG (452)	82	-	2.22	32
Cyclodextrin	5.8	MR (291)	60	MO (327)	93			5.71	-	7
PIM	8.7	SOG (214)	99.9	DR (314)	99.9			1.00	-	33
Conjugated polymers	22.5	AZB (182)	10.2	MB (320)	48.4			1.74	-	34
γ-CDA-TPC-0.1	9.30			MO (327)	60.0	SY (452)	94.5	-	7.27	This work
β-CDA-TPC-0.05	9.84			MO (327)	81.3	SY (452)	98.3	-	11	This work
α-CDA-TPC-0.05	7.64	AZB (182)	33.9	MO (327)	93.0			-	9.44	This work
α-CDA-TPC-0.1-Al	9.51	AZB (182)	18.3	MO (327)	91.3			-	9.39	This work

Abbreviations: MW-molecular weight, COF-covalent organic frameworks, PIM-polymers of intrinsic microporosity, AZB-azobenzene, SOG-sudan orange G, NR-natural red, HNSA-6-hydroxy-2-naphthalenesulfonic acid sodium salt, CSG-chrysoidine G, MR-methyl red sodium salt, DR-disperse red, MB-methylene blue, MO-methyl orange, SO-safranin O, CV-crystal violet, RBB-rhodamine B base, SY-sunset yellow, OG-orange G, PR-primuline, IC-indigo carmine. The molecular weight of each dye was shown in the bracket after the name of the dyes. Selectivity was calculated by following Equation 2.

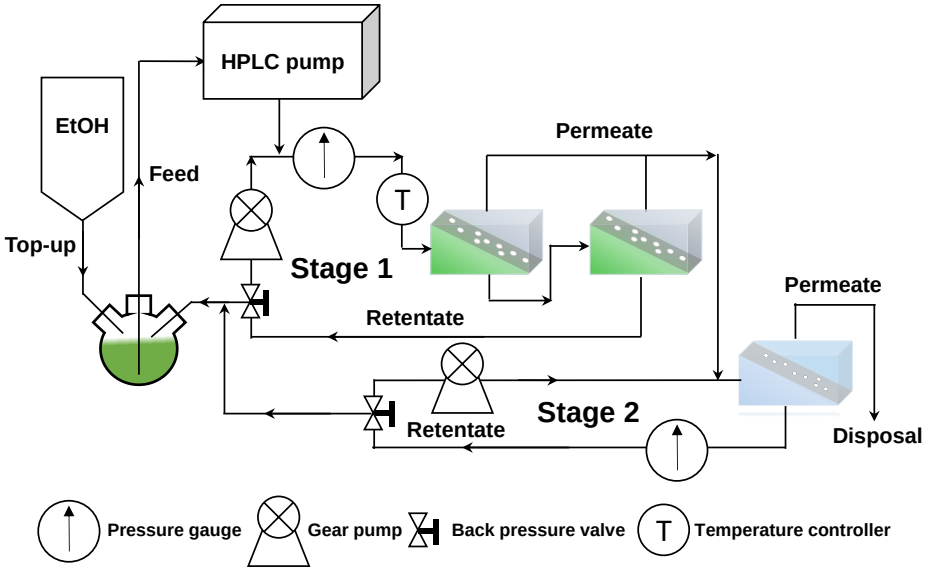

Supplementary Figure 50 | Schematic illustrating a cascade process for enriching CBD.

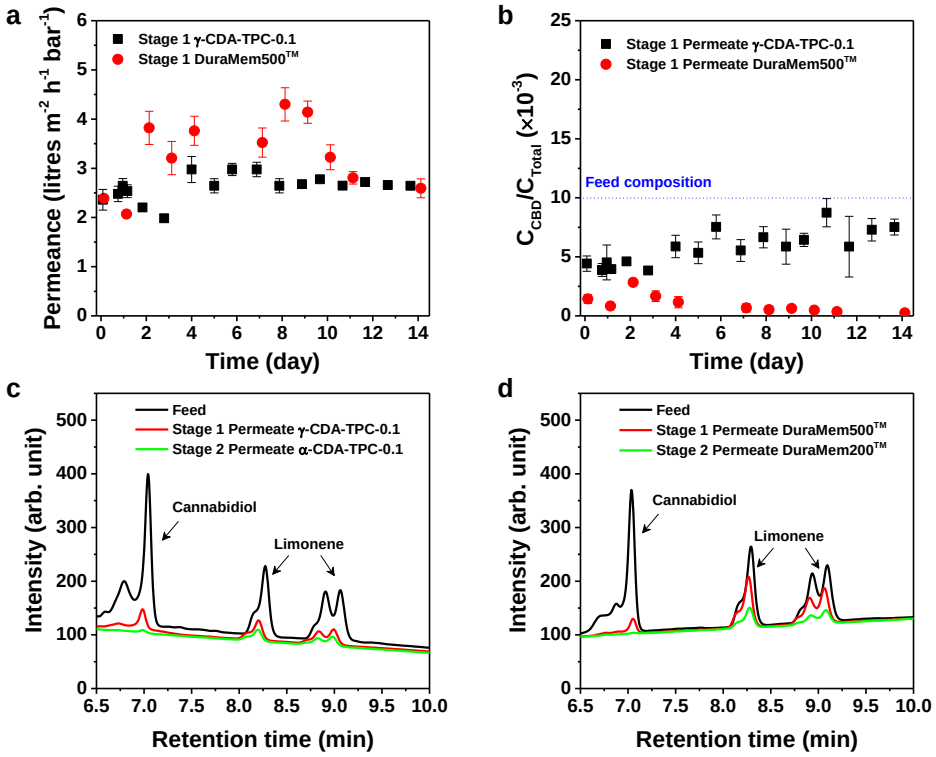

Supplementary Figure 51 | Performance of cascade process enriching CBD. a, Ethanol permeance and **b,** the concentration of CBD in permeate over time for nanofilms incorporating aligned macrocycle pores (*γ*-CDA-TPC-0.1) and commercial standard membrane DuraMem500™ used in Stage 1. Ultra-violet (UV) absorbance of CBD and limonene from high-performance liquid chromatography (HPLC) for **c,** composite membranes incorporating aligned macrocycle pores versus **d,** commercial membranes. Composite membranes comprising large cavity (*γ*-CDA-TPC-0.1) and DuraMem500™ were used at Stage 1 and composite membranes comprising small cavity (*α*-CDA-TPC-0.1) and DuraMem200™ were used at Stage 2.

References

41. Zhao, Q. & Liu, Y., Macrocycle crosslinked mesoporous polymers for ultrafast separation of organic dyes. *Chem. Commun.* **54**, 7362-7365 (2018).

42. van de Manakker, F., Vermonden, T., van Nostrum, C. F. & Hennink, W. E., Cyclodextrin-Based Polymeric Materials: Synthesis, Properties, and Pharmaceutical/Biomedical Applications. *Biomacromolecules* **10**, 3157-3175 (2009).

43. Hansen, C. M., *Hansen Solubility Parameters: A User's Handbook* (CRC Press, Boca Raton, FL, ed. 2, 2007).